

# Holter-to-Sleep: AI-Enabled Repurposing of Single-Lead ECG for Sleep Phenotyping

Donglin Xie<sup>1,2</sup>, Qingshuo Zhao<sup>3</sup>, Jingyu Wang<sup>4</sup>, Shijia Geng<sup>5</sup>, Jiarui Jin<sup>6</sup>, Jun Li<sup>1,2</sup>, Rongrong Guo<sup>4</sup>, Guangkun Nie<sup>1,6</sup>, Gongzheng Tang<sup>1,2</sup>, Yuxi Zhou<sup>3,7</sup>, Thomas Penzel<sup>8,\*</sup>, and Shenda Hong<sup>1,2,9,\*</sup>

<sup>1</sup>National Institute of Health Data Science, Peking University, Beijing, China

<sup>2</sup>Institute of Medical Technology, Peking University Health Science Center, Beijing, China

<sup>3</sup>Department of Computer Science, Tianjin University of Technology, Tianjin, China

<sup>4</sup>Department of Respiratory and Critical Care Medicine, Binzhou Medical University Hospital, Binzhou, China

<sup>5</sup>Heart Voice Medical Technology, Hefei, Anhui

<sup>6</sup>School of Intelligence Science and Technology, Peking University

<sup>7</sup>Department of Respiratory, The Second Hospital of Tianjin Medical University, Tianjin, China

<sup>8</sup>Interdisciplinary Center of Sleep Medicine, Charité - Universitätsmedizin Berlin, Berlin, Germany

<sup>9</sup>Institute for Artificial Intelligence, Peking University, Beijing, China

\*Correspondence: hongshenda@pku.edu.cn, thomas.penzel@charite.de

## ABSTRACT

Sleep disturbances are tightly linked to cardiovascular risk, yet polysomnography (PSG)—the clinical reference standard—remains resource-intensive and poorly suited for multi-night, home-based, and large-scale screening. Single-lead electrocardiography (ECG), already ubiquitous in Holter and patch-based devices, enables comfortable long-term acquisition and encodes sleep-relevant physiology through autonomic modulation and cardiorespiratory coupling. Here, we present a proof-of-concept Holter-to-Sleep framework that, using single-lead ECG as the sole input, jointly supports overnight sleep phenotyping and Holter-grade cardiac phenotyping within the same recording, and further provides an explicit analytic pathway for scalable cardio–sleep association studies. The framework is developed and validated on a pooled multi-center PSG sample of 10,439 studies spanning four public cohorts, with independent external evaluation to assess cross-cohort generalizability, and additional real-world feasibility assessment using overnight patch-ECG recordings via objective–subjective consistency analysis. This integrated design enables robust extraction of clinically meaningful overnight sleep phenotypes under heterogeneous populations and acquisition conditions, and facilitates systematic linkage between ECG-derived sleep metrics and arrhythmia-related Holter phenotypes. Collectively, the Holter-to-Sleep paradigm offers a practical foundation for low-burden, home-deployable, and scalable cardio–sleep monitoring and research beyond traditional PSG-centric workflows.

## KEYWORDS

Holter-to-Sleep, Single-lead ECG, Scalable home sleep phenotyping, Cardio–sleep association analysis

## Introduction

Sleep is a fundamental biological process that sustains systemic homeostasis and is essential for cognitive performance, emotional regulation, and metabolic stability. Persistent sleep disturbances are consistently associated with adverse health outcomes, including cardiovascular disease,

metabolic dysfunction, and neurocognitive impairment<sup>1-7</sup>. Accordingly, scalable and accessible sleep monitoring is increasingly important for both clinical screening and population-level sleep health management.

PSG is widely regarded as the clinical gold standard for sleep assessment. By recording multimodal signals—including electroencephalography (EEG), electrooculography (EOG), electromyography (EMG), respiratory airflow, oxygen saturation, and ECG—PSG enables comprehensive characterization of sleep architecture and sleep-related events, such as arousals and disordered breathing<sup>8-10</sup>. Despite its indispensable role, PSG remains resource-intensive and operationally constrained by specialized equipment, trained personnel, and laborious scoring procedures, limiting its scalability for multi-night monitoring, home deployment, and large-scale screening<sup>11</sup>.

Among candidate modalities for scalable sleep monitoring, single-lead ECG is uniquely positioned to bridge clinical-grade assessment and real-world deployment. Single-lead ECG is already widely available from routine Holter and patch-based wearable devices, supports comfortable long-term recordings at home, and enables continuous, low-burden monitoring across multiple nights. From a physiological perspective, sleep-related autonomic modulation, respiratory load, and arousal responses are reflected in heart rate dynamics and ECG morphology, motivating ECG-based inference of sleep stages and sleep disturbances<sup>12-24</sup>. Importantly, ECG is inherently dual-purpose: if robust sleep characterization can be achieved from the same signal used for cardiac monitoring, a single overnight recording can concurrently provide sleep metrics and Holter-grade cardiac analytics, thereby enabling scalable investigation of cardio-sleep associations.

Prior work has demonstrated the feasibility of ECG-based sleep analysis, spanning conventional feature-based approaches and deep learning models for single-lead ECG sleep staging and sleep event detection<sup>25-33</sup>. In parallel, the rapid growth of wearable sensing has stimulated renewed interest in home sleep monitoring using ECG and other unobtrusive signals<sup>34-36</sup>. Nevertheless, substantial gaps remain before single-lead ECG can serve as a comprehensive and generalizable substrate for scalable sleep monitoring, and these gaps directly motivate the present study. First, many ECG-based studies rely on limited-scale datasets with restricted population diversity, which constrains robustness under cross-cohort distribution shifts<sup>37-39</sup>. Second, sleep is governed by long-range temporal dynamics and structured stage transitions; models that insufficiently capture multi-epoch context may underperform when generalized across centers and cohorts. Third, existing approaches often treat sleep staging, respiratory event detection, and arousal recognition as isolated tasks, preventing shared representation learning and limiting the ability to produce PSG-like holistic outputs. Fourth, external validation and real-world wearable testing remain scarce, leaving uncertainties regarding reliability under practical acquisition conditions. Finally, even when sleep inference is feasible, a systematic pathway to integrate ECG-derived sleep phenotypes with Holter-level arrhythmia analytics for scalable cardio-sleep association studies is largely under-explored.

Here we present a **Holter-to-Sleep** framework that uses single-lead ECG as the sole input to jointly characterize sleep architecture and clinically relevant sleep disturbances at scale, with rigorous multi-cohort validation and real-world wearable assessment, and further enables Holter-level cardio-sleep association analyses. Figure 1 displays an overview of the study, and the key contributions of this study are as follows:

- **Holter-to-Sleep framework:** We establish a Holter-to-Sleep framework demonstrating that single-lead ECG can support holistic sleep characterization for scalable home monitoring.
- **Two-Stage deep learning architecture:** We introduce a Two-Stage deep learning architecture that combines CNN-based morphological representation learning with Transformer-

based temporal refinement to better capture long-range sleep dynamics and improve cross-cohort generalization.

- **Unified multi-task learning:** We develop a Unified multi-task learning strategy that simultaneously models sleep staging and detects key sleep disturbances, aligning model outputs with PSG-style reporting.
- **Multi-cohort validation and wearable assessment:** We conduct multi-center training/internal validation and independent external validation on NSRR cohorts<sup>40–44</sup>, and further perform real-world wearable validation using patch-based ECG with objective–subjective consistency assessment.
- **Holter-level cardio–sleep association analysis:** We perform Holter-level cardio–sleep association analyses by linking ECG-derived sleep phenotypes with arrhythmia-related cardiac phenotypes, providing a scalable analytic pathway for cardio–sleep medicine.

## RESULTS

### PSG cohorts

A total of 10,439 PSG studies were included, and single-lead ECG was extracted from each record as the model input. The combined MESA<sup>42</sup>, MrOS<sup>43</sup>, and SHHS<sup>44</sup> cohorts ( $n = 9,730$ ) were used for model development and internal evaluation, and were split into a training set ( $n = 6,811$ ), a training-validation set ( $n = 1,460$ ), and an internal validation set ( $n = 1,459$ ). The CFS cohort served as an independent external validation set ( $n = 709$ ). Table 1 summarizes demographics and PSG-derived sleep and event-burden metrics for each split (continuous variables reported as mean $\pm$ s.d.; categorical variables reported as  $n$  (%)). The external cohort differs from the development cohorts in age/sex composition and several sleep-related indices, providing an independent setting for assessing cross-cohort generalizability.

### Consistent sleep staging and epoch-level sleep event detection performance with strong cross-cohort generalization

To assess cross-cohort generalizability, we evaluated the proposed model on the held-out internal validation set from MESA/MrOS/SHHS and the independent external validation cohort (CFS). Confusion matrices for four staging granularities are shown in Figure 2, and the corresponding quantitative metrics with 95% confidence intervals (CIs) are summarized in Table 2. In 4-class staging (W/Light/Deep/REM), the model achieved  $\kappa = 0.701$  [0.700, 0.702] on internal validation and  $\kappa = 0.744$  [0.743, 0.745] on external validation (Macro AUC: 0.944 [0.944, 0.944] and 0.959 [0.959, 0.959], respectively). For sleep disturbance detection, ROC curves are shown in Figure 3 and performance metrics with 95% CIs are reported in Table 3. Arousal detection achieved an AUC of 0.855 [0.855, 0.856] on internal validation and 0.864 [0.863, 0.865] on external validation, while respiratory event detection achieved an AUC of 0.787 [0.786, 0.788] and 0.785 [0.784, 0.787], respectively.

To provide qualitative context for single-lead ECG sleep staging, we curated representative ECG-based sleep-staging studies and summarized their reported datasets, PSG sample sizes, and headline metrics in Appendix C. Because cohorts, label sets, and evaluation protocols vary across studies, this summary is intended for context rather than head-to-head benchmarking;

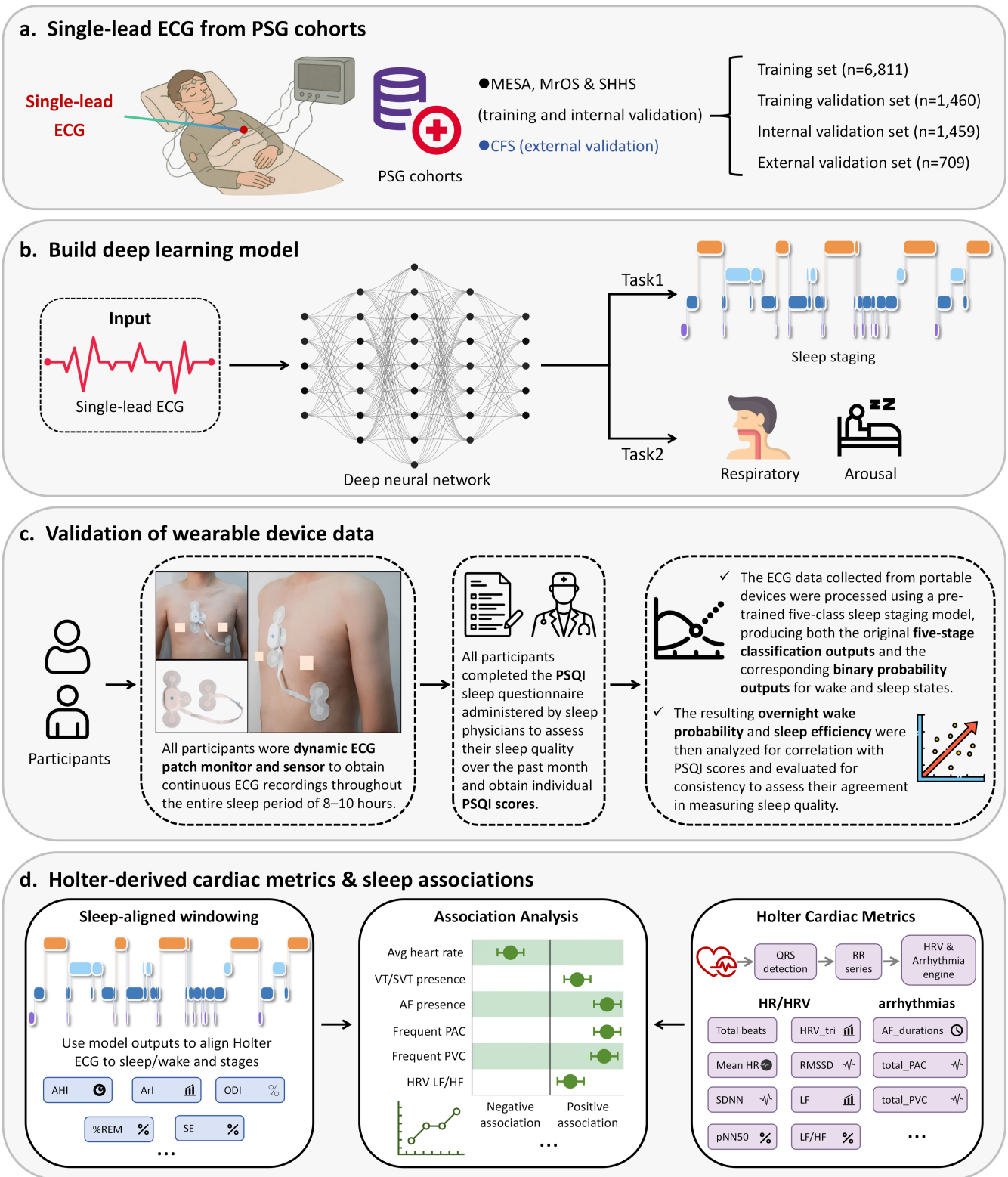


Figure 1: **Overview of the Holter-to-Sleep study design and analytic workflow.** **a**, Data collection. Single-lead ECG was extracted from multi-center PSG cohorts. **b**, Model development. ECG-based deep learning model for sleep staging and sleep disturbance detection. **c**, Wearable data validation. Participants underwent overnight recordings using a patch-based ECG device, accompanied by PSQI-based subjective sleep quality assessment; model-derived sleep-consistency metrics were used to evaluate real-world agreement. **d**, Holter-derived cardiac metrics and sleep associations. Model outputs were used to align long-duration nocturnal ECG with sleep, enabling joint extraction of sleep metrics and Holter-grade cardiac phenotypes, followed by association analyses to support scalable cardio–sleep phenotyping.

Table 1: **Baseline characteristics and PSG-derived sleep metrics across data splits.** Continuous variables are reported as mean±s.d.; categorical variables are reported as *n* (%). AHI, apnea-hypopnea index; Ari, arousal index; ODI, oxygen desaturation index; TST, total sleep time; TIB, time in bed; WASO, wake after sleep onset.

Metric	Training ( <i>n</i> = 6,811)	Train-val ( <i>n</i> = 1,460)	Internal val ( <i>n</i> = 1,459)	External val ( <i>n</i> = 709)
<b>Demographics</b>				
Age (years)	68.48±10.89	68.38±11.20	68.72±10.56	41.34±19.45
Female, <i>n</i> (%)	2,354 (34.56%)	496 (33.97%)	495 (33.93%)	388 (54.72%)
BMI (kg m <sup>-2</sup> )	27.94±4.84	28.04±4.87	28.02±4.91	32.12±9.26
<b>Event burden and oxygen desaturation</b>				
AHI (events h <sup>-1</sup> )	20.21±17.02	20.39±17.41	20.22±16.98	12.30±16.75
Ari (events h <sup>-1</sup> )	16.49±6.68	16.46±6.68	16.33±6.24	12.75±6.07
ODI 3% (events h <sup>-1</sup> )	6.41±9.74	6.62±9.80	6.43±9.67	6.43±12.50
ODI 4% (events h <sup>-1</sup> )	3.71±7.18	3.91±7.34	3.74±7.20	4.07±9.46
<b>Sleep architecture (percentage of TST)</b>				
N1 / TST (%)	7.81±6.71	7.88±6.62	8.05±6.89	5.14±4.94
N2 / TST (%)	58.50±11.28	58.91±11.18	58.42±11.47	56.08±13.07
N3 / TST (%)	14.45±11.24	13.94±11.14	14.18±11.24	21.20±13.77
NREM / TST (%)	80.76±6.59	80.73±6.61	80.65±6.53	82.42±7.27
REM / TST (%)	19.24±6.59	19.27±6.61	19.35±6.53	17.58±7.27
<b>Sleep continuity and fragmentation</b>				
TIB (min)	528.69±84.83	527.74±84.38	527.70±84.87	535.92±49.52
TST (min)	352.73±67.33	351.86±67.44	353.77±65.08	353.34±70.88
Sleep efficiency (%)	68.02±15.14	67.93±15.09	68.29±14.62	66.24±13.32
Wake / TIB (%)	31.98±15.14	32.07±15.09	31.71±14.62	33.76±13.32
Sleep latency (min)	53.31±57.80	55.74±58.21	53.41±59.39	98.67±68.77
WASO (min)	84.76±61.99	83.24±62.61	83.48±60.82	76.47±60.79

Table 2: **Cross-cohort performance for ECG-based sleep staging at multiple granularities.** Values are reported as point estimates with 95% CIs in brackets. For 4-class staging, Light merges N1+N2 and Deep corresponds to N3; for 3-class staging, NREM merges N1–N3; for 2-class staging, Sleep merges N1–N3 and REM.

Class setting	Accuracy $\uparrow$	Weighted F1 $\uparrow$	Kappa $\uparrow$	Macro AUC $\uparrow$
<b>Internal validation</b>				
5-class	0.773 [0.772, 0.773]	0.761 [0.760, 0.762]	0.670 [0.668, 0.670]	0.930 [0.930, 0.930]
4-class	0.804 [0.803, 0.804]	0.801 [0.801, 0.802]	0.701 [0.700, 0.702]	0.944 [0.944, 0.944]
3-class	0.870 [0.869, 0.870]	0.869 [0.869, 0.870]	0.776 [0.775, 0.777]	0.962 [0.962, 0.962]
2-class	0.926 [0.926, 0.926]	0.926 [0.926, 0.926]	0.834 [0.834, 0.835]	0.974 [0.974, 0.975]
<b>External validation (CFS)</b>				
5-class	0.812 [0.811, 0.813]	0.801 [0.800, 0.802]	0.729 [0.728, 0.731]	0.946 [0.945, 0.946]
4-class	0.826 [0.825, 0.827]	0.822 [0.821, 0.822]	0.744 [0.743, 0.745]	0.959 [0.959, 0.959]
3-class	0.892 [0.891, 0.893]	0.892 [0.891, 0.893]	0.814 [0.813, 0.815]	0.975 [0.974, 0.975]
2-class	0.924 [0.923, 0.924]	0.925 [0.924, 0.925]	0.833 [0.832, 0.834]	0.978 [0.977, 0.978]

likewise, we did not compile cross-study comparisons for sleep-event detection given substantial heterogeneity in event definitions, time scales, and disorder taxonomies. 129 130

## ECG emerges as a promising modality for scalable sleep staging after channel-wise comparison 131 132

To contextualize the role of single-lead ECG in sleep staging and quantify the benefit of the proposed two-stage model, CNN with Transformer-based temporal refinement, we performed a channel-wise comparison on the CFS cohort (Table 4). Adding the Transformer consistently improved staging performance across all channels relative to the CNN-only (Net1D) baseline. Notably, for ECG-2,  $\kappa$  increased from 0.621 to 0.748 (a 20.45% relative increase), with Accuracy=0.823, Weighted F1=0.819, and Macro AUC=0.949. Under single-channel settings, ECG-2 approached the performance of channels more directly associated with sleep staging, while the multimodal reference set (C4+LOC+EMG1) achieved the highest overall performance. 133 134 135 136 137 138 139 140

## Real-world wearable data validation: ECG-derived sleep consistency metrics correlate with PSQI 141 142

In the patch-based wearable ECG cohort, epoch-level PSG labels were unavailable. We therefore evaluated real-world consistency by comparing model-derived overnight metrics with subjective sleep quality assessed by the Pittsburgh Sleep Quality Index (PSQI)<sup>45</sup>(Fig. 4). Specifically, wake probability was defined as the overnight mean of epoch-wise wake probabilities, and sleep efficiency was estimated from model-inferred sleep–wake information. In  $n = 26$  participants, wake probability was positively correlated with normalized PSQI ( $r = 0.61, p = 1.02 \times 10^{-3}$ ), whereas sleep efficiency was negatively correlated with normalized PSQI ( $r = -0.43, p = 2.96 \times 10^{-2}$ ). 143 144 145 146 147 148 149

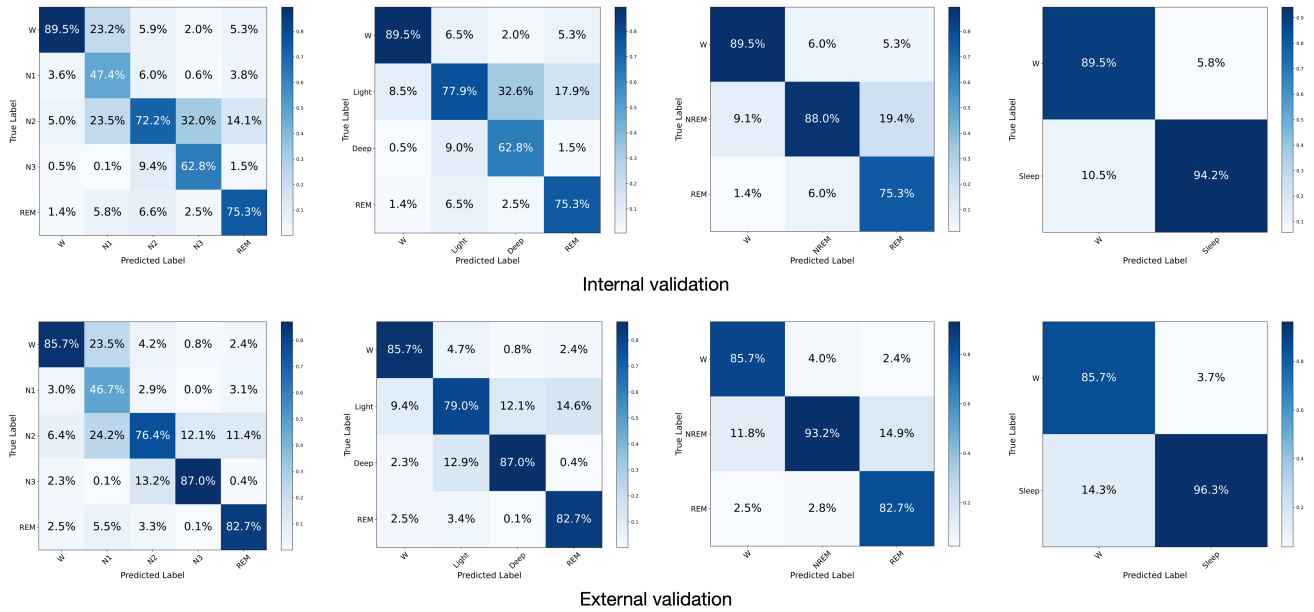


Figure 2: **Cross-cohort generalization of single-lead ECG sleep staging on internal and external validation.** The top row shows internal validation and the bottom row shows external validation; from left to right are confusion matrices for 5-class, 4-class, 3-class, and 2-class staging. Each cell reports the epoch count, with the percentage in parentheses normalized by the predicted class. For 4-class staging, Light merges N1+N2 and Deep corresponds to N3; for 3-class staging, NREM merges N1–N3; for 2-class staging, Sleep merges N1–N3 and REM.

Table 3: **Cross-cohort performance for ECG-based sleep event detection.** Values are reported as point estimates with 95% CIs in brackets. AUC, area under the receiver operating characteristic curve.

Metric	Arousal	Respiratory
<b>Internal validation</b>		
Accuracy ↑	0.852 [0.852, 0.853]	0.798 [0.798, 0.799]
Precision ↑	0.518 [0.517, 0.520]	0.368 [0.366, 0.369]
Recall ↑	0.593 [0.591, 0.595]	0.534 [0.532, 0.536]
Specificity ↑	0.899 [0.899, 0.900]	0.843 [0.843, 0.844]
F1-score ↑	0.553 [0.552, 0.555]	0.435 [0.434, 0.437]
AUC ↑	0.855 [0.855, 0.856]	0.787 [0.786, 0.788]
<b>External validation (CFS)</b>		
Accuracy ↑	0.895 [0.894, 0.895]	0.838 [0.837, 0.839]
Precision ↑	0.558 [0.554, 0.561]	0.301 [0.298, 0.304]
Recall ↑	0.555 [0.552, 0.558]	0.465 [0.461, 0.469]
Specificity ↑	0.940 [0.940, 0.941]	0.880 [0.879, 0.880]
F1-score ↑	0.556 [0.553, 0.559]	0.365 [0.363, 0.368]
AUC ↑	0.864 [0.863, 0.865]	0.785 [0.784, 0.787]

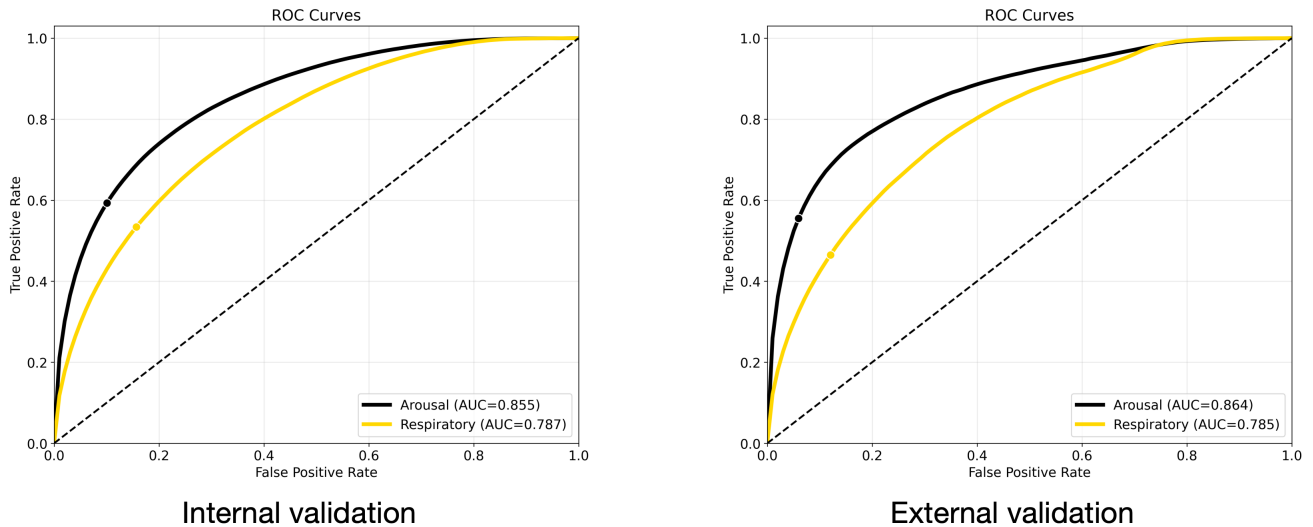


Figure 3: **Cross-cohort generalization of sleep event detection.** ROC curves are shown for arousal and respiratory event detection; the left panel corresponds to internal validation and the right panel to external validation. The area under the ROC curve (AUC) is reported in each panel.

Table 4: **Channel-wise comparison on the CFS cohort highlights ECG as a competitive modality for scalable sleep staging.** Performance is reported for 5-class sleep staging using individual PSG channels. Net1D denotes the CNN-only baseline, and CNN+Trans denotes the proposed two-stage model with temporal refinement. Relative  $\kappa$  increase is computed as  $(\kappa_{\text{CNN+Trans}} - \kappa_{\text{CNN}}) / \kappa_{\text{CNN}} \times 100\%$ .

Channel	Method	Accuracy $\uparrow$	Weighted F1 $\uparrow$	$\kappa$ $\uparrow$	Macro AUC $\uparrow$	Relative $\kappa$ increase
C4+LOC+EMG1	Net1D	0.843	0.842	0.782	0.962	–
	Net1D+Trans	0.886	0.881	0.838	0.977	+7.16%
EEG-C4	Net1D	0.827	0.822	0.759	0.955	–
	Net1D+Trans	0.873	0.869	0.820	0.974	+8.04%
EOG-L	Net1D	0.832	0.829	0.767	0.956	–
	Net1D+Trans	0.878	0.875	0.826	0.975	+7.69%
EMG1	Net1D	0.705	0.690	0.580	0.880	–
	Net1D+Trans	0.787	0.778	0.700	0.936	+20.69%
ECG-2	Net1D	0.725	0.718	0.621	0.903	–
	Net1D+Trans	0.823	0.819	0.748	0.949	+20.45%
Airflow	Net1D	0.482	0.459	0.247	0.694	–
	Net1D+Trans	0.632	0.610	0.454	0.836	+83.81%

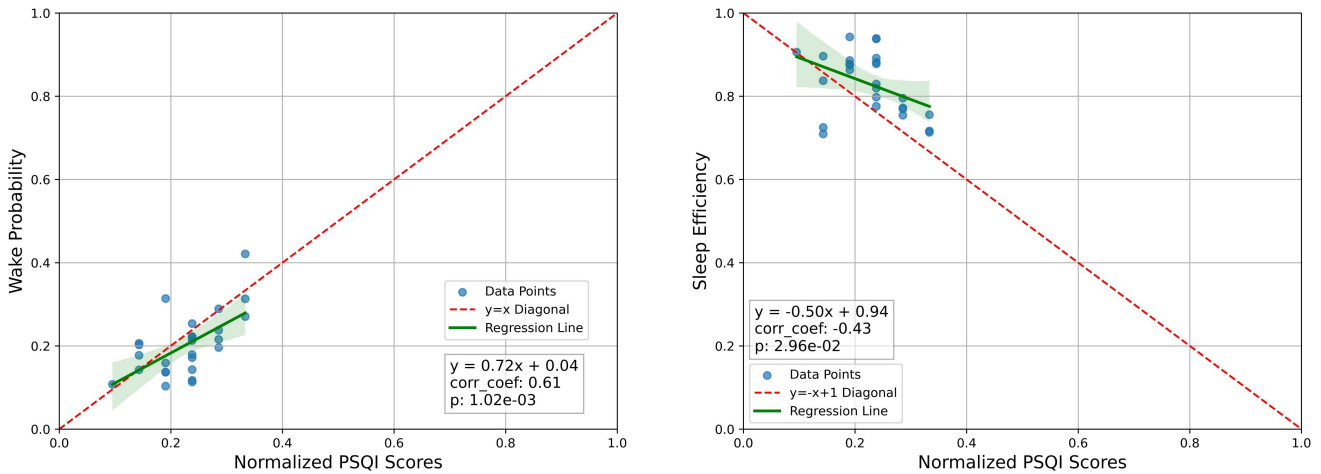


Figure 4: **Real-world wearable validation of ECG-derived sleep consistency metrics against PSQI.** Scatter plots show associations between normalized PSQI scores and model-derived overnight metrics. **Left:** wake probability, defined as the overnight mean of epoch-wise predicted wake probabilities. **Right:** sleep efficiency estimated from model-inferred sleep–wake information. Solid lines indicate linear regression with 95% confidence bands. Pearson's correlation coefficient ( $r$ ) and two-sided  $p$  values are shown in each panel.

## ECG-derived sleep phenotypes reveal cross-cohort heart–sleep associations

Across the pooled multi-cohort PSG sample, we derived overnight sleep phenotypes from single-lead ECG model inference and compared their distributions across arrhythmia-related strata (Fig. 5). Relative to their corresponding reference groups, individuals with arrhythmia phenotypes or higher ectopy burden consistently exhibited poorer sleep, characterized by longer TIB, longer SL, lower SE, and higher ODI 3%; all stratified comparisons annotated in the figure were statistically significant ( $P < 0.001$ ).

For frequent premature ventricular contraction (PVC), TIB increased from  $529.91 \pm 78.58$  to  $553.12 \pm 81.75$  min, SL increased from  $50.96 \pm 55.26$  to  $68.59 \pm 66.18$  min, SE decreased from  $68.70 \pm 14.25\%$  to  $62.85 \pm 15.07\%$ , and ODI 3% increased from  $6.20 \pm 9.59$  to  $7.58 \pm 10.75$ . For frequent premature atrial contraction (PAC), TIB increased from  $528.92 \pm 78.31$  to  $548.36 \pm 81.56$  min, SL increased from  $50.37 \pm 54.86$  to  $64.31 \pm 63.75$  min, SE decreased from  $69.04 \pm 14.18\%$  to  $63.67 \pm 14.86\%$ , and ODI 3% increased from  $6.00 \pm 9.21$  to  $7.86 \pm 11.61$ . For atrial fibrillation (AF) during sleep, TIB increased from  $530.74 \pm 79.05$  to  $548.11 \pm 79.79$  min, SL increased from  $51.69 \pm 55.96$  to  $63.98 \pm 63.25$  min, SE decreased from  $68.28 \pm 14.52\%$  to  $65.73 \pm 13.87\%$ , and ODI 3% increased from  $6.21 \pm 9.49$  to  $7.56 \pm 11.51$ . For ventricular tachycardia (VT), the differences were more pronounced: TIB increased from  $531.11 \pm 78.86$  to  $564.65 \pm 81.98$  min, SL increased from  $52.04 \pm 56.24$  to  $74.05 \pm 66.62$  min, SE decreased from  $68.23 \pm 14.44\%$  to  $63.26 \pm 14.32\%$ , and ODI 3% increased from  $6.30 \pm 9.72$  to  $7.68 \pm 10.32$ .

Collectively, these results indicate that ECG-inferred sleep phenotypes can robustly capture discriminative sleep differences aligned with Holter-grade arrhythmia phenotypes in a cross-cohort setting. Further subgroup analyses of phenotypes and complete results can be found in the Appendix G.

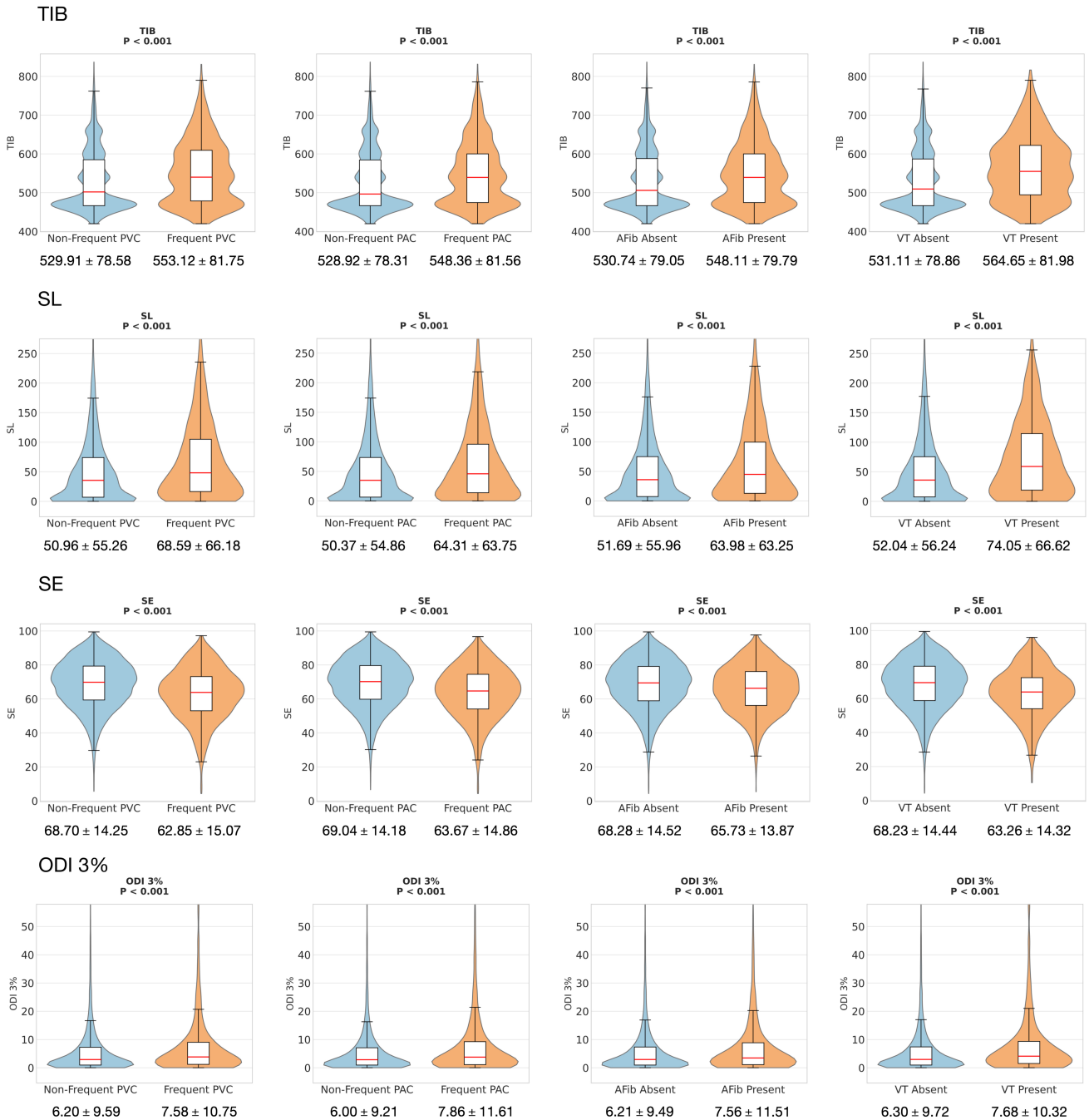


**Figure 5: ECG-derived sleep phenotypes differ across Holter arrhythmia-related strata.** Violin plots show distributions of time in bed (TIB), sleep latency (SL), sleep efficiency (SE), and oxygen desaturation index at 3% (ODI 3%). Participants are stratified by (i) frequent premature ventricular contractions (PVC burden  $\geq 21$  events  $\text{h}^{-1}$ ) versus non-frequent PVC, (ii) frequent premature atrial contractions (PAC burden  $\geq 30$  events  $\text{h}^{-1}$ ) versus non-frequent PAC, (iii) atrial fibrillation (AF) presence during sleep versus absence, and (iv) ventricular tachycardia (VT) presence during sleep versus absence. Embedded boxplots indicate the median and interquartile range. Values below each panel denote mean  $\pm$  s.d.  $P$  values from between-group comparisons are annotated in each panel. TIB and SL are reported in minutes, SE in %, and ODI 3% in events  $\text{h}^{-1}$ .

## From algorithm to application: an integrated web dashboard for ECG-based sleep & Holter cardiac reporting

To facilitate practical use and result interpretation, we implemented an integrated web dashboard that combines ECG-based sleep inference with Holter-grade long-term ECG analytics (Fig. 6). The system accepts raw EDF recordings, automatically parses the ECG channel, and generates a consolidated overnight report including continuous heart-rate trends, a sleep-stage timeline, and summary sleep and cardiac metrics, enabling unified review of nocturnal cardio–sleep phenotypes.

## DISCUSSION

This study proposes and validates a proof-of-concept *Holter-to-Sleep* framework that enables simultaneous sleep phenotyping and Holter-grade cardiac phenotyping using single-lead ECG alone, together with an explicit pathway for downstream cardio–sleep association analyses. In contrast to prior work that typically targets a single sleep task or relies on multi-channel PSG signals, our framework provides a scalable paradigm that integrates nocturnal sleep assessment and cardiac risk characterization within the same data source and workflow. This unified design is particularly relevant to home-based, lightweight, and low-burden monitoring scenarios, and it lays a methodological and engineering foundation for scalable cardio–sleep research, longitudinal health management, and potential screening or follow-up applications.

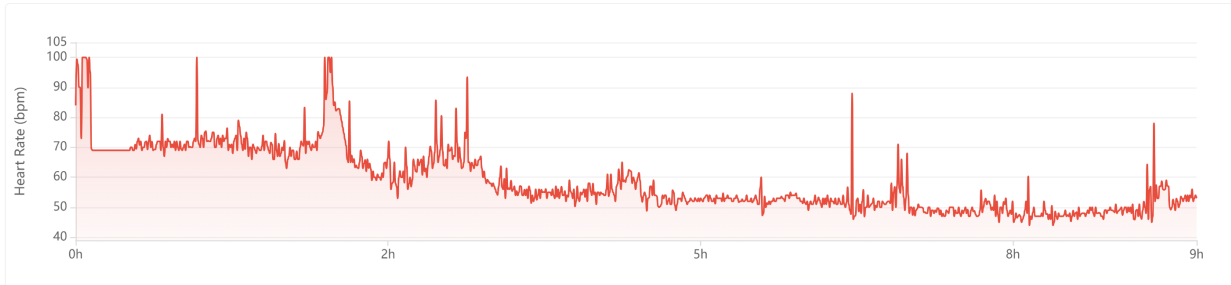
Regarding methodological validity, we systematically evaluated ECG-based sleep staging, arousal detection, and respiratory event detection on multi-center cohorts totaling more than 10,000 PSG studies, and further assessed generalizability via internal validation and an independent external cohort. Although the study is not intended as a head-to-head benchmarking against existing methods, the scale of the data and the consistent cross-cohort performance support that the proposed approach is extensible and transferable across heterogeneous populations, providing a strong basis for deployment in larger cohorts and more complex real-world settings. Algorithmically, the proposed design aims to maximally exploit sleep-relevant physiological information embedded in single-lead ECG. First, we fused time-domain, frequency-domain, and time–frequency representations to enhance sensitivity to autonomic modulation, rhythmic dynamics, and non-stationary components. Second, a CNN backbone captures local morphology and short-term dynamics, while a Transformer module models longer-range temporal dependencies, improving discrimination of sleep architecture and event boundaries. Third, multi-epoch concatenation incorporates contextual information from neighboring epochs and leverages temporal consistency to stabilize epoch-level predictions. Ablation studies in Appendix D indicate that each component contributes to the overall performance.

The channel-wise comparison (Table 4) provides complementary evidence for single-lead ECG as a strong and pragmatic modality for scalable sleep staging from the perspective of sensor availability, information content, and deployability. Under the stringent single-channel setting, ECG-2 with temporal refinement achieved performance close to channels more directly associated with conventional staging (e.g., EEG and EOG), while clearly outperforming respiratory surrogates that are more vulnerable to real-world signal degradation (e.g., airflow). Notably, the relative gain brought by the Transformer was particularly pronounced for ECG, suggesting that stage-related cardiac cues are expressed less as isolated within-epoch patterns and more as temporally structured dynamics—reflecting the minute-scale unfolding of sleep continuity, transition regularities, and autonomic/respiratory modulation of heart-rate fluctuations. This observation motivates the two-stage design adopted in this work: learning robust epoch-level representations while explicitly modeling contextual dependencies and sequence-level constraints

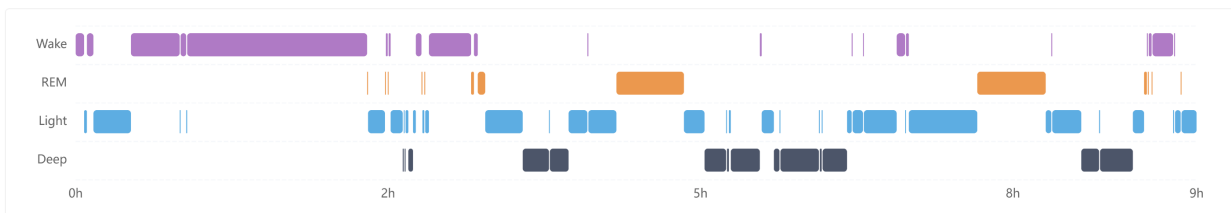
## cfs-visit5-802295.edf - Analysis Report

Analyzed on: 2026-02-27 13:36:44

### Continuous Heart Rate



### Sleep Staging



### Sleep Metrics

Total Recording	Total Sleep
<b>9.97 h</b>	<b>6.88 h</b>
Sleep Efficiency	Wake Ratio
<b>69.06 %</b>	<b>30.94 %</b>
Light Sleep	Deep Sleep
<b>35.03 %</b>	<b>20.07 %</b>
REM Ratio	AHI (Apnea)
<b>13.96 %</b>	<b>17.58</b>
Ari (Arousal)	
<b>8.86</b>	

### Cardiac Metrics

Avg Heart Rate	Min / Max HR
<b>67 bpm</b>	<b>44 / 100 bpm</b>
Total PAC	Total PVC
<b>213</b>	<b>225</b>
AF Events	SVT Events
<b>0</b>	<b>0</b>
VT Events	SDNN
<b>2</b>	<b>255.7 ms</b>
SDANN	RMSSD
<b>216.85 ms</b>	<b>206.16 ms</b>
pNN50	LF Power
<b>7332</b>	<b>10759.09</b>
HF Power	LF/HF Ratio
<b>15071.63</b>	<b>0.71</b>

Figure 6: An integrated web dashboard for ECG-based sleep and Holter cardiac reporting. The dashboard supports raw EDF input, automatically extracts the ECG channel, and integrates the proposed sleep inference pipeline with Holter-grade cardiac analytics. The interface provides (top) an overnight heart-rate trend, (middle) a sleep-stage timeline, and (bottom) summary sleep metrics and cardiac metrics (including HRV and arrhythmia-related summaries) in a consolidated report.

using attention. From a translational standpoint, single-lead ECG is routinely available in PSG and constitutes a standard sensing modality in Holter and patch-based monitors; thus, leveraging ECG enables competitive sleep staging without the additional acquisition burden of dedicated neurophysiological electrodes, supporting longitudinal follow-up and population-scale cardio-sleep phenotyping. We emphasize that multimodal PSG remains the reference standard for maximal diagnostic fidelity; the present work targets cost-effective, scalable screening and phenotyping rather than replacing full clinical polysomnography.

Beyond PSG-based validation, we further examined real-world feasibility using a dynamic ECG patch monitor (HeartVoice, Anhui, China) to acquire overnight recordings in an unconstrained setting. Because epoch-level PSG labels are unavailable in this wearable cohort, we derived interpretable overnight metrics from model outputs (overnight wake probability and sleep efficiency) and evaluated their consistency with subjective sleep quality assessed by the PSQI. The observed associations suggest that the proposed approach can provide informative sleep-related summaries under real-world conditions without PSG supervision, supporting its potential for broader deployment and longitudinal studies.

From a clinical and public health perspective, jointly assessing sleep and cardiac phenotypes is necessary. In the Holter cohort, arrhythmia phenotypes and higher ectopy burden were associated with a consistent pattern of worse sleep, including increased time in bed, prolonged sleep latency, reduced sleep efficiency, and elevated hypoxemia burden. These findings suggest that conventional Holter analyses alone may not fully capture nocturnal physiology, and that incorporating sleep phenotypes within the same monitoring framework can help reveal clinically meaningful interactions and risk signals. A single-lead ECG solution that simultaneously supports sleep and cardiac phenotyping is therefore well aligned with the need for low-burden, home-based, continuous cardio-sleep monitoring.

Several additional strengths are noteworthy. We leveraged multi-center cohorts and performed external validation, supporting reproducibility and scalability. The end-to-end pipeline spans data ingestion, sleep inference, cardiac analytics, association analysis, and reporting, lowering the engineering barrier for translation. Moreover, the implemented web dashboard enables automated parsing of raw EDF recordings and generation of integrated overnight reports, facilitating practical adoption by researchers and clinicians and accelerating translation from proof-of-concept to real-world workflows.

This study also has limitations. First, the wearable validation relied on PSQI as a reference. PSQI is subjective and reflects sleep quality over approximately one month, whereas our ECG recordings covered a single night; thus, the wearable analysis primarily characterizes correlations between single-night model-derived metrics and recent subjective sleep quality rather than strict epoch-level accuracy in real-world sleep staging. Nevertheless, this approach provides a pragmatic starting point for feasibility assessment in the absence of PSG labels. Future work should incorporate multi-night recordings, sleep diaries, and/or additional wearable modalities to strengthen ecological validity. Second, supplementary experiments with cohort-specific training (Appendix A) show reduced performance when training and evaluating on MESA or SHHS alone. This may reflect the higher prevalence of cardiovascular comorbidities in these cohorts, leading to more complex and heterogeneous ECG morphologies and rhythms that challenge learning of stable sleep-relevant representations within a single cohort. Future directions include comorbidity-aware stratification, domain adaptation, and explicit robustness mechanisms for arrhythmias and noise to improve performance in high-risk populations.

In summary, by using single-lead ECG as the sole input, we establish an extensible Holter-to-Sleep framework that supports multi-task sleep inference, integrates Holter-grade cardiac phenotyping, and enables cardio-sleep association analyses, providing a feasible pathway toward low-burden, home-based continuous cardio-sleep monitoring.

# METHODS

269

## Datasets and data preprocessing

270

### Datasets and data annotation

271

In our study, we assembled a unified dataset for model development, validation, and real-world evaluation by integrating single-lead ECG signals from four large public PSG cohorts and by collecting additional long-term wearable ECG recordings. The public cohorts included MESA, MrOS, SHHS, and CFS. MESA, MrOS, and SHHS were used for model training and internal validation, whereas CFS served as an independent external validation cohort. Real-world wearable data were acquired using a patch-based dynamic ECG monitor, yielding 70 overnight recordings; after questionnaire completion and quality control, these data were used for real-world consistency evaluation. To ensure data quality and cross-cohort comparability, we applied unified inclusion/exclusion criteria with quality control on monitoring duration and sleep-stage distributions. The complete screening process and cohort-specific sample sizes are summarized in Fig. 7.

272  
273  
274  
275  
276  
277  
278  
279  
280  
281

We strictly aligned single-lead ECG signals extracted from PSG with the corresponding sleep annotations by parsing XML annotation files matched to the EDF recordings. Three 30-s epoch-level label sequences were generated for each record: sleep staging labels, arousal event labels, and respiratory event labels. Sleep stages followed standard 30-s scoring with Wake, N1, N2, N3, and REM; for consistency, N3 and N4 annotations were merged into N3. Arousal labels were defined as a binary sequence, where an epoch was labeled as 1 if any arousal event occurred within the 30-s window and 0 otherwise. Respiratory labels were also defined in a binary manner: an epoch was labeled as 1 if hypopnea or any apnea event (obstructive, central, or mixed) occurred within the 30-s window, and 0 otherwise. To ensure complete temporal coverage and accurate signal-label alignment, we computed the total number of 30-s epochs for each PSG recording and constructed label sequences of equal length accordingly. Because the beginning and end of recordings are often affected by device setup/termination and signal instability, we excluded the first and last 60 epochs (approximately 60 minutes in total; 30 minutes at each end) from each ECG record to mitigate boundary noise. Ultimately, each recording yielded a time-aligned signal matrix together with sleep stage, arousal, and respiratory event labels for downstream modeling and analysis.

282  
283  
284  
285  
286  
287  
288  
289  
290  
291  
292  
293  
294  
295  
296  
297

### Data preprocessing

298

A standardized preprocessing pipeline was applied to single-lead ECG signals extracted from PSG recordings to improve signal quality and cross-dataset consistency, including resampling, filtering, baseline correction, and normalization. All ECG signals were first resampled to 100 Hz to remove sampling-rate variability across cohorts. A 0.5–40 Hz bandpass filter was then used to suppress low-frequency drift and high-frequency noise, preserving the principal ECG components. Baseline drift was subsequently corrected by fitting and removing a first-order polynomial, thereby reducing slow baseline fluctuations associated with electrode contact variation or motion. To enhance comparability across recordings, robust Z-score normalization was performed to attenuate the influence of outliers. Finally, amplitude normalization linearly scaled each standardized signal to the range  $[-1, 1]$ , mitigating inter-record amplitude discrepancies and providing uniform inputs for downstream model training.

299  
300  
301  
302  
303  
304  
305  
306  
307  
308  
309

## Construction of frequency and time–frequency features

310

The neural network input comprises two components: the time-domain ECG waveform and a set of frequency and time–frequency features. The time-domain waveform corresponds to a 30-s segment. For each 30-s segment, the Power Spectral Density (PSD) was first estimated using the Welch method. By segmenting the signal, applying windowing, and performing the Fourier transform, Welch’s approach reduces the influence of noise on spectral estimation and yields frequency components with their corresponding spectral power. Based on the estimated spectrum, nine physiologically relevant frequency-domain features were extracted. Specifically, band powers in Delta (0.5–4 Hz), Theta (4–8 Hz), and Alpha (8–13 Hz) ranges were computed to characterize energy distribution across bands, and total spectral power was calculated to reflect the overall energy level. The peak frequency was obtained as the frequency with the maximum spectral power. In addition, the spectral centroid (power-weighted mean frequency) and spectral bandwidth (standard deviation around the centroid) were computed to summarize the center and spread of the spectral distribution. Spectral shape was further quantified using spectral flatness, where higher flatness indicates a more noise-like spectrum, and spectral entropy was computed on the normalized spectrum to quantify randomness and complexity.

Time–frequency features were additionally derived using wavelet transforms to capture localized signal characteristics across multiple time and frequency scales. Wavelet analysis provides multi-resolution representations and is well suited for non-stationary physiological signals. In this study, a Daubechies wavelet (db4) was adopted as the basis function, and a four-level Discrete Wavelet Transform (DWT) was applied to each 30-s ECG segment, yielding five sets of coefficients: approximation coefficients at level 5 and detail coefficients at levels 1–4. For each coefficient level, energy (sum of squared coefficients) was computed to quantify scale-specific energy contributions. Furthermore, statistical descriptors, including mean, standard deviation, variance, maximum, and minimum, were extracted to characterize amplitude variation and local morphology across scales. Finally, the nine frequency-domain features and the 30 wavelet-derived time–frequency features were concatenated to form a 39-dimensional handcrafted feature vector; the complete feature list is provided in Appendix F.

## Development of deep learning model

338

We propose a two-stage deep learning framework that takes single-lead ECG as input and jointly performs sleep staging and sleep event detection (Fig. 8). The overall design follows a representation learning–temporal refinement paradigm. Stage 1 employs a CNN to learn robust morphology- and rhythm-related representations from each 30-s epoch, and fuses them with frequency/time–frequency descriptors to form a unified feature vector. Stage 2 freezes the Stage 1 feature extractor and uses a Transformer to model multi-epoch context, improving temporal consistency and boundary discrimination for the center epoch.

**Stage 1: CNN representation learning with multi-domain feature fusion.** For each preprocessed 30-s single-lead ECG epoch, the time-domain signal is fed into a 1D CNN (Net1D) backbone—adapted from the architecture proposed by Hong *et al.*<sup>46</sup>—to capture morphological and rhythmic patterns, yielding a high-dimensional deep representation. Concurrently, the corresponding frequency-domain features are projected into a compatible embedding space. The deep representation and the handcrafted spectral/time–frequency embeddings are then fused at the feature level to obtain a shared representation for downstream predictions.

**Task formulation: sleep staging and multi-task event detection.** Using the shared representation, sleep staging is formulated as a five-class classification task. For sleep events, we adopt a shared-weight multi-task learning head to simultaneously detect arousals and respiratory-related events, leveraging potential physiological relatedness across tasks and improving training

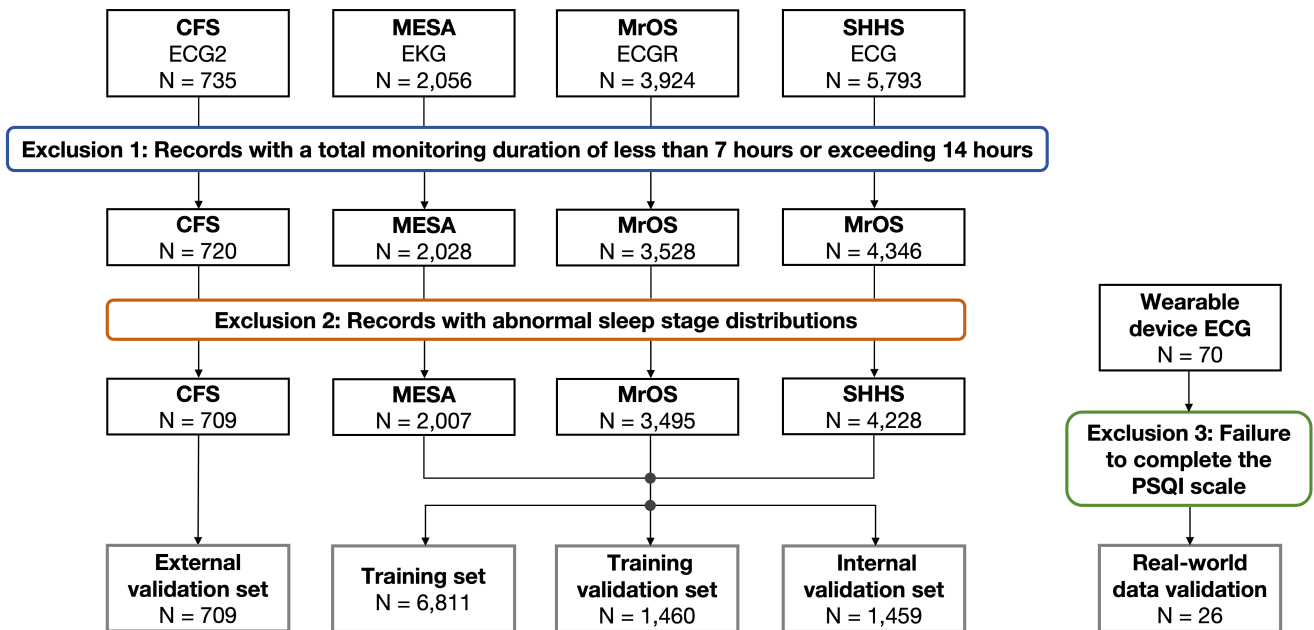


Figure 7: **Study dataset construction and screening flow.** Public PSG cohorts included CFS (ECG2,  $N = 735$ ), MESA (EKG,  $N = 2056$ ), SHHS (ECG,  $N = 5793$ ), and MrOS (ECGR,  $N = 3924$ ). **Exclusion 1:** recordings with total monitoring duration  $< 7$  h or  $> 14$  h; remaining samples were CFS  $N = 720$ , MESA  $N = 2028$ , SHHS  $N = 4346$ , and MrOS  $N = 3528$ . **Exclusion 2:** recordings with abnormal sleep-stage distributions; remaining samples were CFS  $N = 709$ , MESA  $N = 2007$ , SHHS  $N = 4228$ , and MrOS  $N = 3495$ . CFS was used as an independent external validation set ( $N = 709$ ). MESA, SHHS, and MrOS were pooled and split into a training set ( $N = 6811$ ), a training-validation set ( $N = 1460$ ), and an internal validation set ( $N = 1459$ ). For real-world wearable ECG,  $N = 70$  recordings were collected; **Exclusion 3:** failure to complete the PSQI questionnaire; the final real-world validation subset comprised  $N = 26$ .

efficiency. Outputs from Stage 1 can be directly used as initial predictions. 357

**Stage 2: Transformer-based temporal refinement.** To exploit the temporal continuity 358  
inherent in sleep architecture, we construct a sliding window of neighboring 30-s epochs. The 359  
feature sequence extracted from Stage 1 is fed into a Transformer encoder to predict the label 360  
of the center epoch<sup>47</sup>. During Stage 2, the Stage 1 CNN feature extractor is frozen, and only 361  
the Transformer and its prediction heads are optimized. This paradigm enables the model to 362  
retain robust local representations while significantly enhancing long-range dependency modeling 363  
and stage-transition awareness. This temporal refinement strategy is applied to both sleep 364  
staging and sleep-event detection. Specifically, the sleep staging task leverages the sequential 365  
context of the epoch-level embeddings, while event detection is formulated as a multitask learning 366  
problem utilizing a shared Transformer encoder with parallel classification heads for the binary 367  
tasks. Both tasks employ a fixed-length local context window and perform classification based 368  
on the representation of the center token. Detailed model architectures and hyperparameters 369  
are provided in Appendix D. The refined outputs from this stage serve as the final predictions for 370  
evaluation, derived-metric computation, and subsequent downstream analyses. 371

**Training objective and loss functions.** No specialized loss engineering was introduced 372  
beyond standard classification objectives. Sleep staging is optimized using the categorical 373  
cross-entropy loss: 374

$$L_{\text{sleep}} = - \sum_{i=1}^5 y_i \log(\hat{y}_i) \quad (1) \quad 374$$

where  $y_i$  and  $\hat{y}_i$  denote the one-hot ground-truth label and the predicted probability for class  $i$ , 375  
respectively. For sleep event detection, a multi-task optimization strategy is adopted, where the 376  
overall loss is the sum of the arousal loss and the respiratory-event loss: 377

$$L_{\text{multi-task}} = L_{\text{arousal}} + L_{\text{respiratory}} \quad (2) \quad 377$$

## Data splitting, thresholding, and uncertainty estimation 378

Train/validation/test splits were created at the recording level, such that all epochs from the same 379  
overnight recording were confined to a single split; the default split ratio was 70%/15%/15% 380  
with a fixed random seed for reproducibility. For multiclass sleep staging, discrete labels were 381  
obtained by argmax over softmax probabilities. For binary event detection, decision thresholds 382  
were determined on the validation set via a grid search (100 equally spaced candidates in 383  
 $t \in [0.01, 0.99]$ ) by maximizing the F1-score and were then fixed for test evaluation. Metric 384  
uncertainty was quantified using nonparametric bootstrap; the resampling unit was the epoch 385  
(30-s segment), with 1000 bootstrap replicates and 95% confidence intervals. 386

## Evaluation metrics 387

Model performance was evaluated using task-appropriate classification metrics for sleep staging 388  
and sleep event detection. For sleep staging, we report overall Accuracy, Weighted F1-score, 389  
Cohen’s Kappa ( $\kappa$ ), and macro-averaged ROC AUC (Macro AUC). Kappa is used as a primary 390  
staging metric to quantify agreement between predictions and reference annotations while 391  
accounting for class imbalance. For sleep event detection (binary classification for arousal and 392  
respiratory events), we report Accuracy, Precision, Recall, Specificity, F1-score, and ROC AUC, 393  
where AUC serves as the primary indicator of discriminative performance. To quantify the stability 394  
and uncertainty of the reported results, 95% confidence intervals (95% CI) for key metrics were 395  
computed using bootstrapping. 396

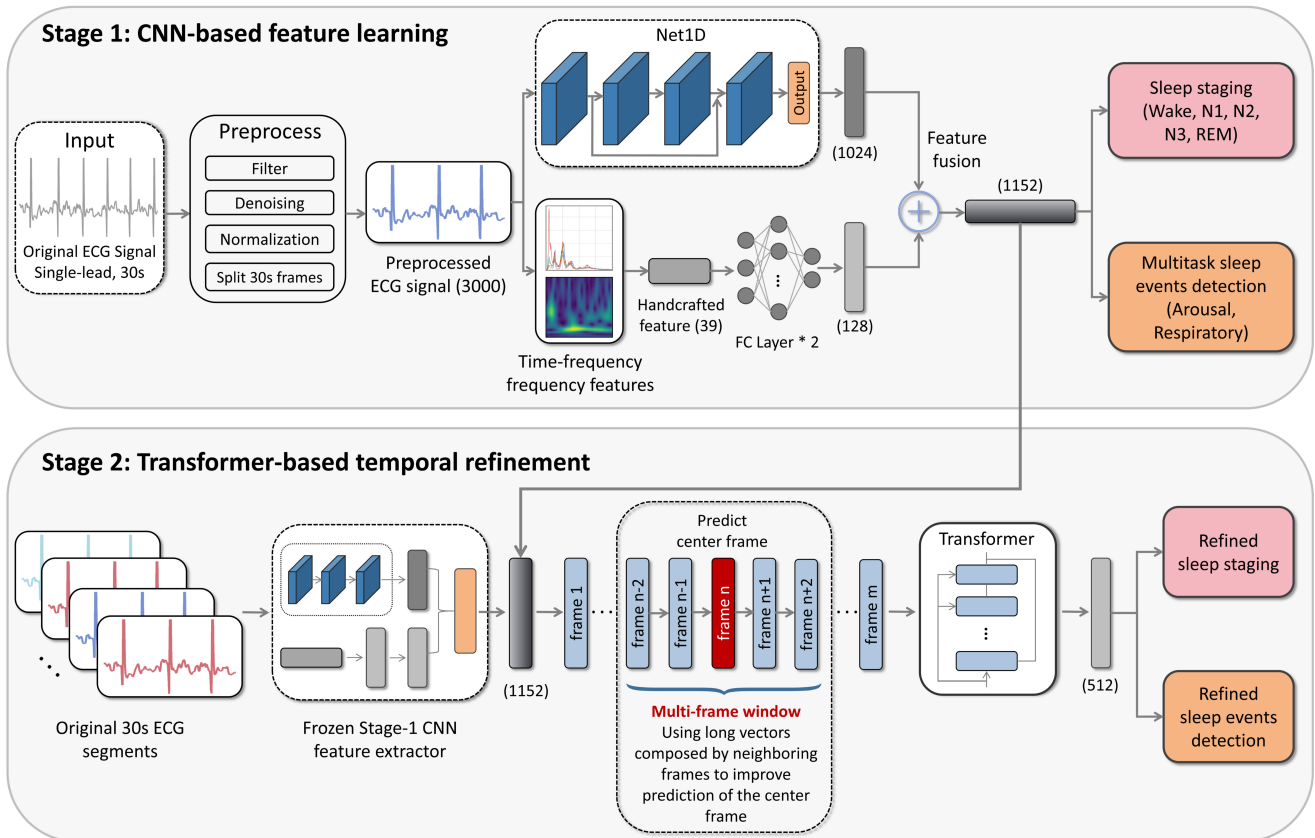


Figure 8: **Two-stage single-lead ECG framework for sleep staging and event detection.** Stage 1 takes 30-s single-lead ECG epochs as input. After preprocessing, a 1D CNN (Net1D) learns deep representations. Frequency/time–frequency features are also extracted and embedded, and then fused with CNN features to produce a shared representation for five-class sleep staging and multi-task sleep event detection, yielding initial predictions. Stage 2 constructs a multi-epoch window from neighboring epochs and feeds the sequence of Stage 1 features into a Transformer. The Stage 1 feature extractor is frozen, and the Transformer performs temporal refinement by predicting the center epoch, producing refined sleep staging and event detection outputs.

## Real-world validation of sleep consistency using wearable ECG data

397

To validate the feasibility of the proposed algorithm in real-world sleep monitoring, we conducted a consistency analysis experiment using wearable single-lead ECG devices. The wake probability throughout the night was used as a surrogate metric for sleep quality, and the relationship between this model-derived metric and self-reported PSQI scores was assessed to evaluate the consistency between algorithmic predictions and subjective sleep quality perceptions. A total of 70 healthy participants were recruited for this study. Each participant wore a dynamic single-lead ECG patch for continuous overnight ECG recording. The following morning, participants were asked to complete the PSQI, which assesses subjective sleep quality on a scale from 0 to 21, with higher scores indicating poorer sleep quality. Complete PSQI questionnaires were obtained from 26 participants, who were included in the PSQI-related analyses.

398

399

400

401

402

403

404

405

406

407

Since single-lead ECG does not provide manual PSG-equivalent annotations, the sleep monitoring algorithm first classified 30-second ECG segments into five sleep stages. To compute the probability of wakefulness across the entire night, we extracted the predicted wake probability from the softmax output of the five-class model for each segment, regardless of its final class label. The per-segment wake probability is denoted as:

408

409

410

411

412

$$P_{\text{Wake},i} = \text{softmax}_{\text{Wake}}(x_i) \quad (3)$$

where  $x_i$  represents the input to the model for the  $i$ -th 30-second epoch, and  $P_{\text{Wake},i}$  denotes the wake probability of the  $i$ -th 30-second segment. The average wake probability over the entire night was computed as:

413

414

415

$$P_{\text{Wake}} = \frac{1}{N} \sum_{i=1}^N P_{\text{Wake},i} \quad (4)$$

where  $N$  represents the total number of 30-second windows during the night. To align the wake probability range with the PSQI scoring scale, the PSQI scores were normalized by dividing by 21. This normalized PSQI score was then used for consistency analysis.

416

417

418

Additionally, we introduced SE as an additional metric, calculated by summing the total duration of non-wake states over the entire night and dividing by the total monitoring duration. Both the normalized PSQI score and the model-derived metrics were then analyzed for consistency.

419

420

421

To evaluate the relationship between the two model-derived metrics—wake probability and SE—and PSQI scores, the Pearson correlation coefficient ( $r$ ) and p-value were computed to quantify their linear association. Furthermore, a least squares regression model was fitted for each metric, and a 95% confidence interval was calculated to assess the robustness of the regression analysis:

422

423

424

425

426

$$y = a \times PSQI_{\text{normalized}} + b \quad (5)$$

where  $y$  denotes the model-derived metric,  $a$  is the regression slope, and  $b$  is the intercept. The full PSQI questionnaire can be found in Appendix H.

427

428

## Joint analysis of Holter-level cardiac metrics and sleep metrics

429

To assess the associations between ECG-derived sleep phenotypes and Holter-level cardiac phenotypes, we constructed two synchronized feature sets for each PSG recording: a sleep-metric set and a cardiac-metric set. The sleep-metric set comprised 16 variables capturing sleep-disordered breathing burden, arousal burden, and sleep architecture/efficiency. The cardiac-metric set

430

431

432

433

comprised 32 Holter-level variables including heart-rate summary statistics, supraventricular/ventricular ectopy burden and rhythm-event summaries, as well as time- and frequency-domain heart-rate variability (HRV) features. Holter-level metric computation followed established practice and was implemented by adapting prior validated pipelines, with specific reference to the CardioLearn framework by Hong *et al.*<sup>48</sup> and the implementation described by Fu *et al.*<sup>49</sup>. Full metric definitions are provided in Appendix E.

We then performed joint analysis using a cardiac-phenotype–stratified comparison strategy, in which sleep phenotypes were compared across groups defined by cardiac phenotypes. Two grouping schemes were used depending on the cardiac variable type: (1) binary/event-based stratification—for rhythm events or indicator variables (e.g., atrial fibrillation (AF) occurrence during sleep and ventricular tachycardia (VT) occurrence), participants were stratified into event-present vs. event-absent groups; and (2) threshold-based burden stratification—for quantitative burden metrics (e.g., premature atrial contractions (PACs) and premature ventricular contractions (PVCs)), event counts were normalized to an hourly rate (events/h), and participants were stratified into “frequent” vs. “non-frequent” groups using predefined thresholds. Consistent with the Results, frequent PVC was defined as a PVC burden  $\geq 21$  events/h and frequent PAC as a PAC burden  $\geq 30$  events/h.

For each stratification, we conducted between-group statistical comparisons of sleep metrics to identify sleep features most strongly associated with cardiac phenotypes. Two-sided tests were applied for continuous sleep metrics, and significance levels were reported. Distributions were visualized using box/violin plots. This workflow enables systematic screening of sleep-phenotype differences anchored to Holter-level cardiac phenotypes within a unified PSG cohort, thereby characterizing clinically meaningful cardio–sleep associations.

## Web dashboard for integrated sleep–cardiac reporting

To facilitate practical usability assessment and result visualization, we integrated the proposed ECG-based sleep analysis model with the Holter-level cardiac metric computation module into a user-facing web dashboard. The system allows users to upload EDF (European Data Format) files and select the target single-lead ECG channel. It then automatically performs signal ingestion and quality control, segmentation and preprocessing, model inference, and the computation and aggregation of sleep and cardiac metrics, ultimately generating an overnight integrated sleep–cardiac report. The report includes an overnight heart-rate trend, a sleep-stage timeline, key sleep and arousal/respiratory metrics. The implementation of the dashboard and the end-to-end pipeline are provided in the public repository: <https://github.com/xd11216/Holter-to-Sleep>.

## RESOURCE AVAILABILITY

467

### Data availability

468

The public sleep cohorts analyzed during the current study are available in the National Sleep Research Resource (NSRR) repository at <https://sleepdata.org/>.

469

470

### Code availability

471

The code for the Holter-to-Sleep framework and the integrated web dashboard are available at <https://github.com/xd11216/Holter-to-Sleep> and <https://github.com/PKUDigitalHealth/Holter-to-Sleep>.

472

473

474

## ACKNOWLEDGMENTS

475

This work was supported by the National Natural Science Foundation of China (62102008, 62172018), CCF-Tencent Rhino-Bird Open Research Fund (CCF-Tencent RAGR20250108), CCF-Zhipu Large Model Innovation Fund (CCF-Zhipu202414), PKU-OPPO Fund (BO202301, BO202503), Research Project of Peking University in the State Key Laboratory of Vascular Homeostasis and Remodeling (2025-SKLVHR-YCTS-02), Beijing Municipal Science and Technology Commission (Z251100000725008). The authors thank all collaborators and participating institutions for their support and contributions to this research.

476

477

478

479

480

481

482

## AUTHOR CONTRIBUTIONS

483

Donglin Xie conceived and designed the study and implemented the algorithms and software. Qingshuo Zhao integrated, curated, and preprocessed the datasets. Jingyu Wang planned the real-world ECG data collection protocol and provided clinical guidance. Shijia Geng and Rongrong Guo prepared the ECG acquisition devices, performed the real-world ECG recordings, and collected PSQI questionnaires. Jiarui Jin, Jun Li, Guangkun Nie and Gongzheng Tang assisted with result interpretation and manuscript revision. Yuxi Zhou contributed to methodological discussions and manuscript editing. Thomas Penzel and Shenda Hong supervised the project, provided overall technical guidance, and critically revised the manuscript. All authors reviewed and approved the final manuscript.

484

485

486

487

488

489

490

491

492

## DECLARATION OF INTERESTS

493

The authors declare no competing interests.

494

## References

1. Barone, M.T., and Menna-Barreto, L. (2011). Diabetes and sleep: a complex cause-and-effect relationship. *Diabetes research and clinical practice* 91, 129–137. 495  
496  
497
2. Lal, C., Strange, C., and Bachman, D. (2012). Neurocognitive impairment in obstructive sleep apnea. *Chest* 141, 1601–1610. 498  
499
3. Hargens, T.A., Kaleth, A.S., Edwards, E.S., and Butner, K.L. (2013). Association between sleep disorders, obesity, and exercise: a review. *Nature and science of sleep* pp. 27–35. 500  
501
4. Vandekerckhove, M., and Wang, Y.I. (2017). Emotion, emotion regulation and sleep: An intimate relationship. *AIMS neuroscience* 5, 1. 502  
503
5. Vyazovskiy, V.V. (2015). Sleep, recovery, and metaregulation: explaining the benefits of sleep. *Nature and science of sleep* pp. 171–184. 504  
505
6. Zisapel, N. (2007). Sleep and sleep disturbances: biological basis and clinical implications. *Cellular and Molecular Life Sciences* 64, 1174–1186. 506  
507
7. Wang, Y., Wen, Q., Luo, S., Tang, L., Zhan, S., Cao, J., Wang, S., and Chen, Q. (2025). Phenome-wide analysis of diseases in relation to objectively measured sleep traits and comparison with subjective sleep traits in 88,461 adults. *Health data science* 5, 0161. 508  
509  
510
8. Van de Water, A.T., Holmes, A., and Hurley, D.A. (2011). Objective measurements of sleep for non-laboratory settings as alternatives to polysomnography—a systematic review. *Journal of sleep research* 20, 183–200. 511  
512  
513
9. Roebuck, A., Monasterio, V., Geder, E., Osipov, M., Behar, J., Malhotra, A., Penzel, T., and Clifford, G. (2013). A review of signals used in sleep analysis. *Physiological measurement* 35, R1. 514  
515  
516
10. Mazzotti, D.R., Lim, D.C., Sutherland, K., Bittencourt, L., Mindel, J.W., Magalang, U., Pack, A.I., De Chazal, P., Penzel, T. et al. (2018). Opportunities for utilizing polysomnography signals to characterize obstructive sleep apnea subtypes and severity. *Physiological measurement* 39, 09TR01. 517  
518  
519  
520
11. De Zambotti, M., Goldstein, C., Cook, J., Menghini, L., Altini, M., Cheng, P., and Robillard, R. (2024). State of the science and recommendations for using wearable technology in sleep and circadian research. *Sleep* 47, zsad325. 521  
522  
523
12. Sun, H., Ganglberger, W., Panneerselvam, E., Leone, M.J., Quadri, S.A., Goparaju, B., Tesh, R.A., Akeju, O., Thomas, R.J., and Westover, M.B. (2020). Sleep staging from electrocardiography and respiration with deep learning. *Sleep* 43, zsz306. 524  
525  
526
13. Wei, R., Zhang, X., Wang, J., and Dang, X. (2018). The research of sleep staging based on single-lead electrocardiogram and deep neural network. *Biomedical engineering letters* 8, 87–93. 527  
528  
529
14. Wei, Y., Qi, X., Wang, H., Liu, Z., Wang, G., and Yan, X. (2019). A multi-class automatic sleep staging method based on long short-term memory network using single-lead electrocardiogram signals. *IEEE Access* 7, 85959–85970. 530  
531  
532

15. Li, Q., Li, Q., Cakmak, A.S., Da Poian, G., Bliwise, D.L., Vaccarino, V., Shah, A.J., and Clifford, G.D. (2021). Transfer learning from ecg to ppg for improved sleep staging from wrist-worn wearables. *Physiological measurement* 42, 044004. 533  
534  
535
16. Zhao, R., Xia, Y., and Wang, Q. (2021). Dual-modal and multi-scale deep neural networks for sleep staging using eeg and ecg signals. *Biomedical Signal Processing and Control* 66, 102455. 536  
537  
538
17. Utomo, O.K., Surantha, N., Isa, S.M., and Soewito, B. (2019). Automatic sleep stage classification using weighted elm and pso on imbalanced data from single lead ecg. *Procedia Computer Science* 157, 321–328. 539  
540  
541
18. Tripathi, P., Ansari, M., Gandhi, T.K., Mehrotra, R., Heyat, M.B.B., Akhtar, F., Ukwuoma, C.C., Muaad, A.Y., Kadah, Y.M., Al-Antari, M.A. et al. (2022). Ensemble computational intelligent for insomnia sleep stage detection via the sleep ecg signal. *IEEE Access* 10, 108710–108721. 542  
543  
544  
545
19. Urtnasan, E., Park, J.U., Joo, E.Y., and Lee, K.J. (2022). Deep convolutional recurrent model for automatic scoring sleep stages based on single-lead ecg signal. *Diagnostics* 12, 1235. 546  
547
20. Lesmana, T.F., Isa, S.M., and Surantha, N. (2018). Sleep stage identification using the combination of elm and pso based on ecg signal and hrv. In *2018 3rd International Conference on Computer and Communication Systems (ICCCS)*. IEEE pp. 258–262. 548  
549  
550
21. Tang, M., Zhang, Z., He, Z., Li, W., Mou, X., Du, L., Wang, P., Zhao, Z., Chen, X., Li, X. et al. (2022). Deep adaptation network for subject-specific sleep stage classification based on a single-lead ecg. *Biomedical Signal Processing and Control* 75, 103548. 551  
552  
553
22. Li, Q., Li, Q., Liu, C., Shashikumar, S.P., Nemat, S., and Clifford, G.D. (2018). Deep learning in the cross-time frequency domain for sleep staging from a single-lead electrocardiogram. *Physiological measurement* 39, 124005. 554  
555  
556
23. Bozkurt, F., Uçar, M.K., Bilgin, C., and Zengin, A. (2021). Sleep–wake stage detection with single channel ecg and hybrid machine learning model in patients with obstructive sleep apnea. *Physical and Engineering Sciences in Medicine* 44, 63–77. 557  
558  
559
24. Zhu, H., Luo, Q., Wang, Y., Maimaiti, M., Zhang, H., Xiong, Y., Ruan, C., Wang, J., Liu, Y., Zhou, M. et al. (2026). Artificial intelligence-enabled 8-channel ecg diagnosing of abnormalities with wide qrs complexes: a cohort study. *Health Data Science*. 560  
561  
562
25. Plesinger, F., Viscor, I., Nejedly, P., Andrla, P., Halamek, J., and Jurak, P. (2018). Automated sleep arousal detection based on eeg envelopograms. In *2018 Computing in Cardiology Conference (CinC)* vol. 45. IEEE pp. 1–4. 563  
564  
565
26. Li, A., Chen, S., Quan, S.F., Powers, L.S., and Roveda, J.M. (2020). A deep learning-based algorithm for detection of cortical arousal during sleep. *Sleep* 43, zsa120. 566  
567
27. Mack, D.C., Alwan, M., Turner, B., Suratt, P., and Felder, R.A. (2006). A passive and portable system for monitoring heart rate and detecting sleep apnea and arousals: Preliminary validation. In *1st Transdisciplinary Conference on Distributed Diagnosis and Home Healthcare, 2006. D2H2*. IEEE pp. 51–54. 568  
569  
570  
571

28. Ragnarsdóttir, H., Marinósson, B., Finnsson, E., Gunnlaugsson, E., Ágústsson, J.S., Helgadóttir, H. et al. (2018). Automatic detection of target regions of respiratory effort-related arousals using recurrent neural networks. In 2018 Computing in Cardiology Conference (CinC) vol. 45. IEEE pp. 1–4. 572  
573  
574  
575
29. Song, C., Liu, K., Zhang, X., Chen, L., and Xian, X. (2015). An obstructive sleep apnea detection approach using a discriminative hidden markov model from ecg signals. IEEE Transactions on Biomedical Engineering 63, 1532–1542. 576  
577  
578
30. Bahrami, M., and Forouzanfar, M. (2022). Sleep apnea detection from single-lead ecg: A comprehensive analysis of machine learning and deep learning algorithms. IEEE Transactions on Instrumentation and Measurement 71, 1–11. 579  
580  
581
31. Varon, C., Caicedo, A., Testelmans, D., Buyse, B., and Van Huffel, S. (2015). A novel algorithm for the automatic detection of sleep apnea from single-lead ecg. IEEE transactions on biomedical engineering 62, 2269–2278. 582  
583  
584
32. Mendonca, F., Mostafa, S.S., Ravelo-Garcia, A.G., Morgado-Dias, F., and Penzel, T. (2018). A review of obstructive sleep apnea detection approaches. IEEE journal of biomedical and health informatics 23, 825–837. 585  
586  
587
33. Radha, M., Fonseca, P., Moreau, A., Ross, M., Cerny, A., Anderer, P., Long, X., and Aarts, R.M. (2019). Sleep stage classification from heart-rate variability using long short-term memory neural networks. Scientific reports 9, 14149. 588  
589  
590
34. Kwon, S., Kim, H., and Yeo, W.H. (2021). Recent advances in wearable sensors and portable electronics for sleep monitoring. Iscience 24. 591  
592
35. Kwon, S., Kim, H.S., Kwon, K., Kim, H., Kim, Y.S., Lee, S.H., Kwon, Y.T., Jeong, J.W., Trotti, L.M., Duarte, A. et al. (2023). At-home wireless sleep monitoring patches for the clinical assessment of sleep quality and sleep apnea. Science Advances 9, eadg9671. 593  
594  
595
36. Chen, Z., Lin, M., Chen, F., Lane, N.D., Cardone, G., Wang, R., Li, T., Chen, Y., Choudhury, T., and Campbell, A.T. (2013). Unobtrusive sleep monitoring using smartphones. In 2013 7th International Conference on Pervasive Computing Technologies for Healthcare and Workshops. IEEE pp. 145–152. 596  
597  
598  
599
37. Kemp, B., Zwinderman, A.H., Tuk, B., Kamphuisen, H.A., and Oberye, J.J. (2000). Analysis of a sleep-dependent neuronal feedback loop: the slow-wave microcontinuity of the eeg. IEEE Transactions on Biomedical Engineering 47, 1185–1194. 600  
601  
602
38. Ichimaru, Y., and Moody, G. (1999). Development of the polysomnographic database on cd-rom. Psychiatry and clinical neurosciences 53, 175–177. 603  
604
39. Goldberger, A.L., Amaral, L.A., Glass, L., Hausdorff, J.M., Ivanov, P.C., Mark, R.G., Mietus, J.E., Moody, G.B., Peng, C.K., and Stanley, H.E. (2000). Physiobank, physiotoolkit, and physionet: components of a new research resource for complex physiologic signals. circulation 101, e215–e220. 605  
606  
607  
608
40. Zhang, G.Q., Cui, L., Mueller, R., Tao, S., Kim, M., Rueschman, M., Mariani, S., Mobley, D., and Redline, S. (2018). The national sleep research resource: towards a sleep data commons. Journal of the American Medical Informatics Association 25, 1351–1358. 609  
610  
611

41. Redline, S., Tishler, P.V., Tosteson, T.D., Williamson, J., Kump, K., Browner, I., Ferrette, V., and Krejci, P. (1995). The familial aggregation of obstructive sleep apnea. *American journal of respiratory and critical care medicine* *151*, 682–687. 612  
613  
614
42. Chen, X., Wang, R., Zee, P., Lutsey, P.L., Javaheri, S., Alcántara, C., Jackson, C.L., Williams, M.A., and Redline, S. (2015). Racial/ethnic differences in sleep disturbances: the multi-ethnic study of atherosclerosis (mesa). *Sleep* *38*, 877–888. 615  
616  
617
43. Blackwell, T., Yaffe, K., Ancoli-Israel, S., Redline, S., Ensrud, K.E., Stefanick, M.L., Laffan, A., Stone, K.L., and in Men Study Group, O.F. (2011). Associations between sleep architecture and sleep-disordered breathing and cognition in older community-dwelling men: the osteoporotic fractures in men sleep study. *Journal of the American Geriatrics Society* *59*, 2217–2225. 618  
619  
620  
621  
622
44. Quan, S.F., Howard, B.V., Iber, C., Kiley, J.P., Nieto, F.J., O'Connor, G.T., Rapoport, D.M., Redline, S., Robbins, J., Samet, J.M. et al. (1997). The sleep heart health study: design, rationale, and methods. *Sleep* *20*, 1077–1085. 623  
624  
625
45. Buysse, D.J., Reynolds III, C.F., Monk, T.H., Berman, S.R., and Kupfer, D.J. (1989). The pittsburgh sleep quality index: a new instrument for psychiatric practice and research. *Psychiatry research* *28*, 193–213. 626  
627  
628
46. Hong, S., Xu, Y., Khare, A., Priambada, S., Maher, K., Aljiffry, A., Sun, J., and Tumanov, A. (2020). Holmes: Health online model ensemble serving for deep learning models in intensive care units. In *Proceedings of the 26th ACM SIGKDD International Conference on Knowledge Discovery & Data Mining*. pp. 1614–1624. 629  
630  
631  
632
47. Vaswani, A., Shazeer, N., Parmar, N., Uszkoreit, J., Jones, L., Gomez, A.N., Kaiser, Ł., and Polosukhin, I. (2017). Attention is all you need. *Advances in neural information processing systems* *30*. 633  
634  
635
48. Hong, S., Fu, Z., Zhou, R., Yu, J., Li, Y., Wang, K., and Cheng, G. (2020). Cardiolearn: a cloud deep learning service for cardiac disease detection from electrocardiogram. In *Companion Proceedings of the Web Conference 2020*. pp. 148–152. 636  
637  
638
49. Fu, Z., Hong, S., Zhang, R., and Du, S. (2021). Artificial-intelligence-enhanced mobile system for cardiovascular health management. *Sensors* *21*, 773. 639  
640
50. Goldberger, A.L., Amaral, L., Glass, L., Hausdorff, J.M., Ivanov, P.C., Mark, R.G., Mietus, J.E., Moody, G.B., Peng, C.K., and Stanley, H.E. (2000). Components of a new research resource for complex physiologic signals. *PhysioBank, PhysioToolkit, and Physionet*. 641  
642  
643
51. Kloth, G., Kemp, B., Penzel, T., Schlogl, A., Rappelsberger, P., Trenker, E., Gruber, G., Zeithofer, J., Saletu, B., Herrmann, W. et al. (2001). The siesta project polygraphic and clinical database. *IEEE Engineering in Medicine and Biology Magazine* *20*, 51–57. 644  
645  
646

## Appendix A Cohort-specific training and validation results

647

Table 5: Sleep staging performance when training and validating the model independently within each cohort. (Point estimates with 95% CI).

Cohort	Class	Accuracy $\uparrow$	Weighted F1 $\uparrow$	$\kappa$ $\uparrow$	Macro AUC $\uparrow$
CFS	5-class	0.841 [0.839, 0.843]	0.835 [0.834, 0.837]	0.776 [0.774, 0.779]	0.959 [0.959, 0.960]
	4-class	0.856 [0.854, 0.857]	0.856 [0.854, 0.858]	0.792 [0.789, 0.794]	0.971 [0.971, 0.972]
	3-class	0.910 [0.909, 0.912]	0.911 [0.909, 0.912]	0.845 [0.843, 0.848]	0.981 [0.980, 0.981]
	2-class	0.945 [0.944, 0.946]	0.945 [0.944, 0.946]	0.875 [0.872, 0.877]	0.984 [0.984, 0.985]
MESA	5-class	0.648 [0.647, 0.650]	0.624 [0.623, 0.626]	0.478 [0.477, 0.480]	0.849 [0.848, 0.849]
	4-class	0.699 [0.698, 0.701]	0.686 [0.685, 0.688]	0.518 [0.516, 0.520]	0.864 [0.864, 0.865]
	3-class	0.758 [0.757, 0.760]	0.755 [0.754, 0.757]	0.584 [0.582, 0.587]	0.881 [0.881, 0.882]
	2-class	0.847 [0.846, 0.848]	0.846 [0.845, 0.847]	0.672 [0.670, 0.674]	0.910 [0.909, 0.911]
MrOS	5-class	0.839 [0.838, 0.840]	0.827 [0.826, 0.828]	0.758 [0.757, 0.760]	0.954 [0.954, 0.954]
	4-class	0.863 [0.862, 0.864]	0.863 [0.862, 0.864]	0.788 [0.786, 0.789]	0.970 [0.970, 0.971]
	3-class	0.900 [0.899, 0.900]	0.900 [0.899, 0.901]	0.831 [0.830, 0.832]	0.977 [0.977, 0.977]
	2-class	0.929 [0.928, 0.929]	0.929 [0.928, 0.929]	0.853 [0.852, 0.854]	0.980 [0.980, 0.980]
SHHS	5-class	0.646 [0.645, 0.647]	0.628 [0.626, 0.629]	0.467 [0.465, 0.469]	0.848 [0.848, 0.849]
	4-class	0.672 [0.671, 0.673]	0.663 [0.662, 0.664]	0.486 [0.484, 0.488]	0.862 [0.861, 0.862]
	3-class	0.784 [0.783, 0.785]	0.780 [0.779, 0.781]	0.582 [0.579, 0.584]	0.891 [0.890, 0.892]
	2-class	0.897 [0.896, 0.898]	0.893 [0.892, 0.893]	0.680 [0.678, 0.682]	0.920 [0.919, 0.921]

648

Table 6: **Arousal Detection Performance:** Independent training and validation within each cohort (Point estimates with 95% CI).

Dataset	Accuracy $\uparrow$	Precision $\uparrow$	Recall $\uparrow$	Specificity $\uparrow$	F1-Score $\uparrow$	AUC $\uparrow$
CFS	0.911 [0.910, 0.912]	0.618 [0.611, 0.625]	0.628 [0.621, 0.636]	0.949 [0.947, 0.950]	0.623 [0.618, 0.629]	0.914 [0.912, 0.916]
MESA	0.812 [0.811, 0.813]	0.438 [0.435, 0.441]	0.568 [0.564, 0.571]	0.859 [0.858, 0.860]	0.495 [0.492, 0.498]	0.808 [0.806, 0.809]
MrOS	0.891 [0.890, 0.891]	0.574 [0.571, 0.577]	0.617 [0.615, 0.620]	0.932 [0.931, 0.932]	0.595 [0.592, 0.597]	0.901 [0.901, 0.902]
SHHS	0.843 [0.842, 0.844]	0.551 [0.549, 0.554]	0.622 [0.620, 0.625]	0.891 [0.890, 0.891]	0.585 [0.583, 0.587]	0.854 [0.853, 0.856]

649

Table 7: **Respiratory Event Detection Performance:** Independent training and validation within each cohort (Point estimates with 95% CI).

Dataset	Accuracy $\uparrow$	Precision $\uparrow$	Recall $\uparrow$	Specificity $\uparrow$	F1-Score $\uparrow$	AUC $\uparrow$
CFS	0.868 [0.867, 0.870]	0.325 [0.319, 0.332]	0.490 [0.482, 0.499]	0.904 [0.902, 0.906]	0.391 [0.384, 0.398]	0.841 [0.838, 0.844]
MESA	0.747 [0.746, 0.748]	0.173 [0.171, 0.176]	0.447 [0.442, 0.451]	0.778 [0.777, 0.779]	0.250 [0.247, 0.253]	0.686 [0.683, 0.688]
MrOS	0.861 [0.860, 0.862]	0.237 [0.234, 0.239]	0.390 [0.386, 0.393]	0.899 [0.898, 0.900]	0.295 [0.292, 0.297]	0.793 [0.791, 0.794]
SHHS	0.717 [0.715, 0.718]	0.468 [0.466, 0.470]	0.657 [0.655, 0.659]	0.738 [0.736, 0.739]	0.547 [0.545, 0.548]	0.769 [0.768, 0.770]

650

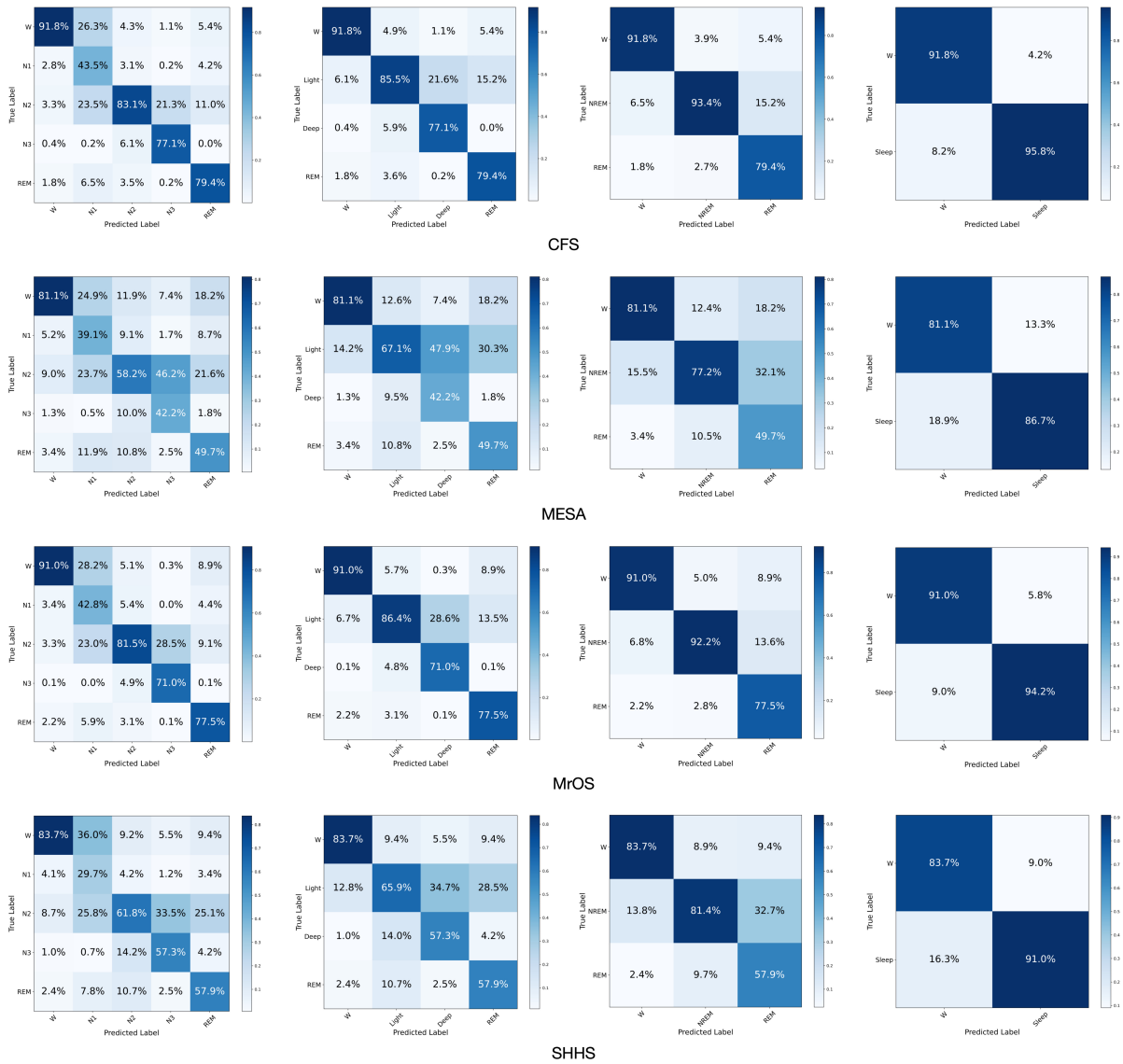
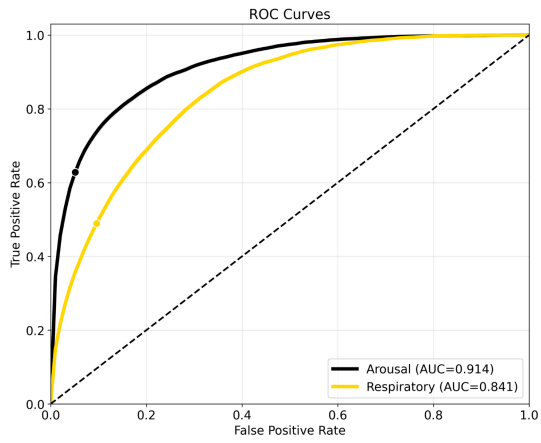
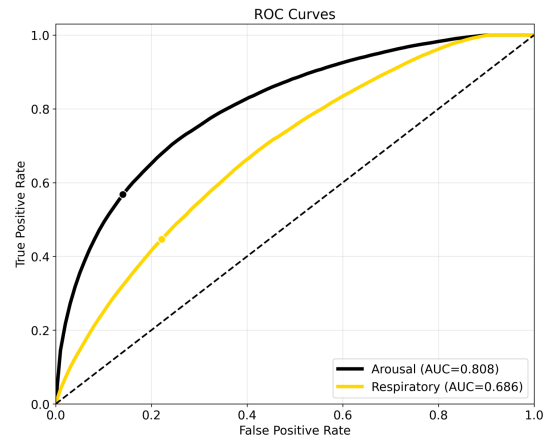


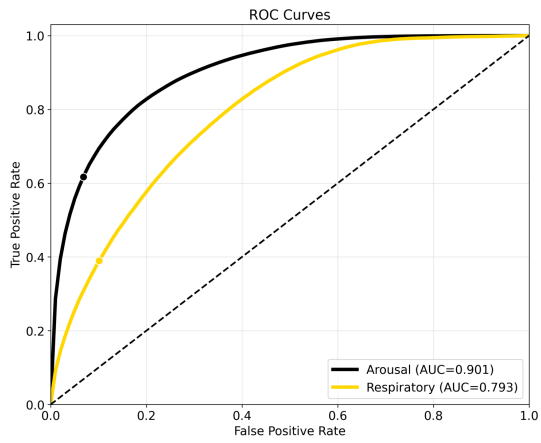
Figure 9: Confusion matrices for cohort-specific sleep staging models.



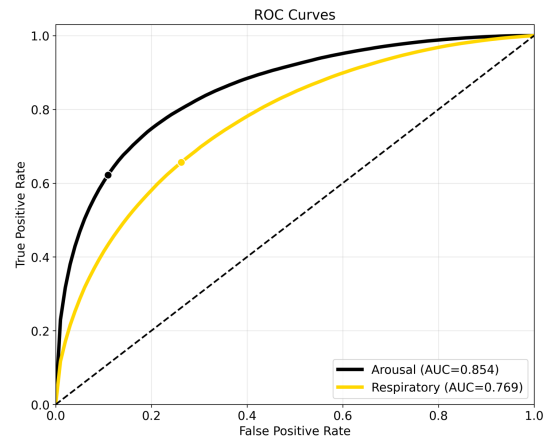
CFS



MESA



MrOS



SHHS

Figure 10: ROC curves for cohort-specific sleep disturbance detection models.

## Appendix B Ablation Study

653

To quantify the contribution of key design choices under a controlled computational budget, all ablation experiments were conducted on the CFS cohort, while keeping the training and evaluation protocol consistent with the main experiments. We investigate (i) feature fusion, (ii) model composition within the two-stage framework, and (iii) the multi-frame window length used by the Transformer-based temporal refinement module.

654

655

656

657

658

### B.1 Feature fusion

659

Table 8: Ablation on feature fusion for sleep staging on CFS. We use the two-stage model, and the Transformer refinement stage adopts multi-frame concatenation with a fixed window size of 15. The comparison evaluates time-domain input only versus feature-level fusion of time-domain representations with frequency/time–frequency descriptors. Feature fusion yields higher  $\kappa$  and improves overall metrics.

Feature Fusion	Accuracy $\uparrow$	Weighted F1 $\uparrow$	$\kappa$ $\uparrow$	Macro AUC $\uparrow$
With Fusion	0.842	0.835	0.776	0.959
Without Fusion	0.823	0.819	0.748	0.949

Table 9: Ablation on feature fusion for multi-task sleep disturbance detection on CFS (arousal and respiratory events). The two-stage model is used, and the Transformer refinement stage adopts a fixed multi-frame window size of 15. Feature fusion improves AUC for both tasks and shows a more pronounced benefit for sleep staging (Table 8).

Feature Fusion	Task	Accuracy $\uparrow$	Precision $\uparrow$	Recall $\uparrow$	Specificity $\uparrow$	F1-Score $\uparrow$	AUC $\uparrow$
With Fusion	Arousal	0.911	0.618	0.628	0.949	0.623	0.914
	Respiratory	0.868	0.325	0.490	0.904	0.391	0.841
Without Fusion	Arousal	0.900	0.569	0.629	0.936	0.597	0.902
	Respiratory	0.847	0.365	0.543	0.884	0.437	0.835

### B.2 Model comparison

660

Table 10: Model comparison for sleep staging on CFS within the proposed two-stage framework. All settings use feature fusion. We compare (i) a stage-1 CNN-only model (Net1D), (ii) a Transformer-only model without the CNN feature extractor, and (iii) the full two-stage model (Net1D + Transformer). For this ablation, the Transformer input window size is fixed to 1 (no multi-frame concatenation).

Model	Accuracy $\uparrow$	Weighted F1 $\uparrow$	$\kappa$ $\uparrow$	Macro AUC $\uparrow$
Net1D	0.735	0.728	0.630	0.912
Transformer	0.756	0.743	0.651	0.912
Net1D + Transformer	0.791	0.780	0.703	0.924

Table 11: Model comparison for multi-task sleep event detection on CFS (arousal and respiratory events). All settings use feature fusion. We compare the stage-1 CNN-only model, a Transformer-only model, and the full two-stage model. For this ablation, the Transformer input window size is fixed to 1 (no multi-frame concatenation).

Model	Task	Accuracy $\uparrow$	Precision $\uparrow$	Recall $\uparrow$	Specificity $\uparrow$	F1-Score $\uparrow$	AUC $\uparrow$
CNN Net1D	Arousal	0.884	0.510	0.563	0.927	0.535	0.868
	Respiratory	0.741	0.192	0.532	0.763	0.283	0.734
Transformer	Arousal	0.705	0.197	0.487	0.734	0.281	0.662
	Respiratory	0.530	0.133	0.711	0.511	0.225	0.647
CNN Net1D + Transformer	Arousal	0.887	0.514	0.602	0.924	0.555	0.878
	Respiratory	0.816	0.302	0.522	0.852	0.383	0.793

### B.3 Multi-frame window size

661

Table 12: Ablation on the multi-frame window length used by the Transformer-based refinement module for sleep staging on CFS. The two-stage model with feature fusion is used, and only the window size is varied from 1 to 21. Performance generally increases as the window length grows, and a window size of 15 provides a strong accuracy–efficiency trade-off without introducing substantial additional computation.

Window size	Accuracy $\uparrow$	Weighted F1 $\uparrow$	$\kappa$ $\uparrow$	Macro AUC $\uparrow$
1	0.791	0.780	0.703	0.924
3	0.824	0.814	0.750	0.945
5	0.833	0.824	0.763	0.951
7	0.838	0.830	0.771	0.955
9	0.841	0.834	0.775	0.958
11	0.836	0.830	0.768	0.956
13	0.839	0.831	0.772	0.956
15	0.842	0.835	0.776	0.959
17	0.842	0.836	0.775	0.958
19	0.842	0.837	0.776	0.959
21	0.838	0.833	0.771	0.957

Table 13: Ablation on the multi-frame window length for multi-task sleep disturbance detection on CFS. The two-stage model with feature fusion is used, and only the Transformer window size is varied from 1 to 21. Overall performance improves as the window length increases, and a window size of 15 provides strong discrimination with limited additional computational overhead.

Window size	Task	Accuracy $\uparrow$	Precision $\uparrow$	Recall $\uparrow$	Specificity $\uparrow$	F1-Score $\uparrow$	AUC $\uparrow$
1	Arousal	0.887	0.514	0.602	0.924	0.555	0.878
	Respiratory	0.816	0.302	0.522	0.852	0.383	0.793
3	Arousal	0.897	0.556	0.625	0.934	0.588	0.899
	Respiratory	0.838	0.344	0.534	0.875	0.418	0.824
5	Arousal	0.903	0.583	0.595	0.944	0.589	0.898
	Respiratory	0.845	0.359	0.529	0.884	0.428	0.827
7	Arousal	0.902	0.578	0.602	0.942	0.590	0.898
	Respiratory	0.849	0.366	0.525	0.889	0.432	0.830
9	Arousal	0.898	0.563	0.606	0.937	0.584	0.895
	Respiratory	0.843	0.357	0.544	0.880	0.431	0.828
11	Arousal	0.898	0.560	0.614	0.936	0.586	0.896
	Respiratory	0.838	0.349	0.563	0.871	0.431	0.830
13	Arousal	0.905	0.592	0.622	0.943	0.607	0.906
	Respiratory	0.850	0.373	0.543	0.888	0.442	0.840
15	Arousal	0.911	0.618	0.628	0.949	0.623	0.914
	Respiratory	0.868	0.325	0.490	0.904	0.391	0.841
17	Arousal	0.902	0.578	0.628	0.939	0.602	0.904
	Respiratory	0.854	0.379	0.517	0.896	0.438	0.837
19	Arousal	0.906	0.597	0.613	0.945	0.605	0.904
	Respiratory	0.857	0.387	0.526	0.897	0.446	0.840
21	Arousal	0.900	0.568	0.618	0.937	0.592	0.898
	Respiratory	0.852	0.374	0.520	0.893	0.435	0.834

## Appendix C Comparison of Existing Studies

Table 14: **Representative single-lead ECG-based sleep-staging studies and their self-reported metrics.** Reported values are taken from the original publications and correspond to each study’s internal test-set evaluation under the label set indicated (3-/4-/5-class).  $N$  denotes the number of PSG recordings unless otherwise specified. Because cohorts, label definitions, and evaluation protocols differ across studies, this table is provided for qualitative context rather than head-to-head benchmarking. Missing entries indicate that the corresponding metric was not reported in the original publication.

Study	Classes	Dataset(s)	$N$	$\kappa$	Acc
Wei <i>et al.</i> (2018) <sup>13</sup>	3	MIT-BIH Polysomnographic Database <sup>50</sup>	18	0.560	0.770
Urtnasan <i>et al.</i> (2022) <sup>19</sup>	3	Private dataset	112	–	0.860
Li <i>et al.</i> (2018) <sup>22</sup>	4	MIT-BIH Polysomnographic Database <sup>50</sup>	18	0.540	0.756
Wei <i>et al.</i> (2019) <sup>14</sup>	4	Xijing Hospital dataset (FMMU)	238	0.550	0.778
Radha <i>et al.</i> (2019) <sup>33</sup>	4	Siesta database <sup>51</sup>	588	0.610	0.770
Sun <i>et al.</i> (2020) <sup>12</sup>	5	MGH Cohort	8682	0.490	–
<b>Holter-to-Sleep (this study)</b>	5	MESA <sup>42</sup> + MrOS <sup>43</sup> + SHHS <sup>44</sup>	9730	0.670	0.773

## Appendix D Supplementary Methods

663

### D.1 Input representation and embedding dimensionality

664

Each 30-s epoch was represented by (i) a time-domain single-lead ECG segment (stored as a 1D vector of length 3000 with an explicit channel dimension) and (ii) an epoch-aligned frequency-domain feature vector (39 dimensions). The epoch-level feature extractor was a Net1D-style architecture with attention-based aggregation for the time-domain backbone output, and a lightweight feed-forward mapping with attention weighting for the frequency-domain features. The final epoch embedding was obtained by concatenating a 1024-dimensional time-domain representation and a 128-dimensional frequency-domain representation, resulting in a 1152-dimensional embedding per epoch.

665  
666  
667  
668  
669  
670  
671  
672

### D.2 Transformer architectures and context-window definition

673

**Sleep-staging Transformer (sequence-level).** The sleep-staging Transformer used a batch-first Transformer Encoder with learnable positional embeddings. For each epoch, we formed a local context window of length  $W = 15$  (7 preceding epochs, the current epoch, and 7 following epochs). The 15 epoch embeddings (each 1152-dimensional) within the window were concatenated to form the input vector of a single token, yielding a token input dimension of  $15 \times 1152$ . The model projected tokens to hidden size  $d = 512$ , added positional embeddings, and applied a  $L = 3$ -layer Transformer Encoder ( $h = 8$  heads, feed-forward dimension  $4d$ , dropout 0.1). The classifier produced 5-class sleep-stage logits for each token in the sequence. Because the number of epochs varies across recordings, sequences were padded within a batch; loss computation ignored padded positions via an `ignore_index` mask.

674  
675  
676  
677  
678  
679  
680  
681  
682  
683

**Sleep-event Transformer (window-level).** For event detection, each local window ( $W = 15$ ) was treated as an individual sample with input shape  $(B, W, 1152)$ . After linear projection to  $d = 512$ , a  $L = 4$ -layer Transformer Encoder ( $h = 8$ , dropout 0.1) generated contextualized hidden states. The center-token representation was used as a shared embedding for two parallel binary classifiers, producing arousal and respiratory logits, respectively.

684  
685  
686  
687  
688

### D.3 Training configuration and hyperparameters

689

**Sleep-staging CNN (epoch-level).** We used Adam with learning rate  $1 \times 10^{-3}$  and weight decay  $1 \times 10^{-5}$ , trained for 50 epochs with batch size 256. A ReduceLROnPlateau scheduler was applied (patience=10, factor=0.3), and early stopping was performed based on validation loss (patience=5). Training supported distributed data parallelism (DDP) and automatic mixed precision (AMP).

690  
691  
692  
693  
694

**Sleep-staging Transformer.** We used Adam with learning rate  $1 \times 10^{-4}$ , batch size 64, and up to 100 epochs, with early stopping based on validation loss (patience=5). The context window length was  $W = 15$  with stride 1. Cross-entropy loss was computed with padded labels ignored by `ignore_index`.

695  
696  
697  
698

**Multitask sleep-event CNN.** The multitask CNN shared a Net1D encoder and used two binary classification heads. We used AdamW with learning rate  $1 \times 10^{-3}$  and weight decay  $1 \times 10^{-5}$ , trained for 50 epochs with batch size 128. ReduceLROnPlateau was applied (patience=5, factor=0.3) with

699  
700  
701

early stopping (patience=3). During training, small additive Gaussian noise (standard deviation 0.01) was used for augmentation. Training supported DDP and AMP. 702  
703

**Sleep-event Transformer.** We used Adam with learning rate  $3 \times 10^{-4}$ , batch size 16, and up to 200 epochs, with early stopping based on validation loss (patience=6). The context window length was  $W = 15$  with stride 1, and logits were computed from the center-token representation using two parallel binary heads. 704  
705  
706  
707

## D.4 Split unit and generation of file lists 708

Train/validation/test splits were performed at the recording-file level (one .npz file per overnight recording). All .npz paths were collected recursively from the specified directories and randomly split with a fixed seed. We first assigned 60% of files to training; the remaining 40% was equally divided into validation and test sets (20%/20%). The resulting file lists were written to train\_paths.txt, val\_paths.txt, and test\_paths.txt. All training and evaluation scripts used these lists as the sole data input, ensuring reproducible splits and results. 709  
710  
711  
712  
713  
714

## D.5 Threshold selection for binary tasks 715

For binary event detection, the model outputs were converted to positive-class probabilities  $p$  via softmax. The decision threshold  $t$  was determined on the validation set by grid search: we evaluated 100 equally spaced candidates in  $t \in [0.01, 0.99]$  and selected the threshold that maximized the F1-score. The selected threshold was then fixed for test evaluation, reporting Accuracy, Precision, Recall, Specificity, F1-score, and AUC. 716  
717  
718  
719  
720

## D.6 Bootstrap unit and confidence intervals 721

We used nonparametric bootstrap to quantify metric uncertainty. The resampling unit was the epoch (30-s segment): the evaluation set was flattened into an epoch-level sample list, which was resampled with replacement for 1000 replicates. For each replicate, the target metric was computed, and the 2.5th and 97.5th percentiles of the bootstrap distribution were used to construct a 95% confidence interval; the bootstrap mean was reported as the point estimate. 722  
723  
724  
725  
726

## Appendix E List of sleep and Holter-grade cardiac metrics

727

For reproducibility and reference, this appendix summarizes the sleep-related metrics (16 items) and Holter-grade cardiac metrics (32 items) used in this study.

728

729

Table 15: Summary of sleep-related metrics and Holter-grade cardiac metrics used in this study.

Sleep metrics (16)	Holter-grade cardiac metrics (32)
AHI (events h <sup>-1</sup> )	Total_valid_beats
Arl (events h <sup>-1</sup> )	Avg_HR
N1 / TST (%)	Min_HR
N2 / TST (%)	Max_HR
N3 / TST (%)	Snt_max_beat_count
NREM / TST (%)	Snt_duration
REM / TST (%)	Snb_max_beat_count
SE (%)	Snb_duration
SL (min)	Total_PAC
TIB (min)	Single_PAC
TST (min)	Paired_PAC
TTSP (min)	Bigeminy_PAC
WASO (min)	Triad_PAC
Wake / TIB (%)	Total_PVC
ODI 3% (events h <sup>-1</sup> )	Single_PVC
ODI 4% (events h <sup>-1</sup> )	Paired_PVC
	Bigeminy_PVC
	Triad_PVC
	Total_VT
	Total_SVT
	SDNN
	SDANN
	SDANNIndex
	RMSSD
	pNN50
	HRV_tri
	LF
	HF
	LFNU
	HFNU
	LF/HF
	AF_duration

# Appendix F Handcrafted frequency and time–frequency features

Table 16: Handcrafted spectral and time–frequency descriptors (39 features) used for feature-level fusion.

Frequency Domain Features	Time-Frequency Features
1. Delta Power	<b>Energy Features:</b> Energy calculated for each wavelet decomposition level (5 levels, first-level coefficients for each level)
2. Theta Power	
3. Alpha Power	<b>Statistical Features:</b> Statistical features computed for each wavelet decomposition level ( $5 \times 5$ matrix, 5 features per decomposition level), including: <ol style="list-style-type: none"> <li>1. Mean</li> <li>2. Standard Deviation</li> <li>3. Variance</li> <li>4. Maximum Value</li> <li>5. Minimum Value</li> </ol>
4. Total Power	
5. Peak Frequency	
6. Spectral Centroid	
7. Spectral Bandwidth	
8. Spectral Flatness	
9. Spectral Entropy	

## Appendix G Detailed tables for joint sleep–Holter stratified analyses

732

733

This appendix reports the complete metric tables used in the joint sleep–Holter stratified analyses. Values are presented as mean  $\pm$  standard deviation. P-values are from two-sided statistical tests; extremely small P-values are reported as “<0.001”, otherwise rounded to three decimals.

734

735

736

### G.1 Frequent PVC vs non-frequent PVC

737

Table 17: Full metric comparison between frequent PVC and non-frequent PVC strata. Values are mean  $\pm$  SD.

Metric	Frequent PVC (n=1,248)	Non-frequent PVC (n=9,191)	P-value
Age (years)	69.83 $\pm$ 14.31	66.29 $\pm$ 12.84	<0.001
BMI (kg m <sup>-2</sup> )	28.51 $\pm$ 5.66	28.25 $\pm$ 5.29	0.250
AHI (events h <sup>-1</sup> )	21.48 $\pm$ 18.03	19.11 $\pm$ 16.86	<0.001
Arl (events h <sup>-1</sup> )	31.36 $\pm$ 18.09	29.13 $\pm$ 15.38	<0.001
N1 % of TST	7.87 $\pm$ 7.10	7.19 $\pm$ 6.23	<0.001
N2 % of TST	59.56 $\pm$ 11.85	58.01 $\pm$ 11.33	<0.001
N3 % of TST	13.93 $\pm$ 11.47	15.22 $\pm$ 11.44	<0.001
NREM % of TST	81.36 $\pm$ 7.17	80.42 $\pm$ 6.57	<0.001
REM % of TST	18.64 $\pm$ 7.17	19.58 $\pm$ 6.57	<0.001
SE (%)	62.85 $\pm$ 15.07	68.70 $\pm$ 14.25	<0.001
SL (min)	68.59 $\pm$ 66.18	50.96 $\pm$ 55.26	<0.001
TIB (min)	553.12 $\pm$ 81.75	529.91 $\pm$ 78.58	<0.001
TST (min)	342.80 $\pm$ 77.32	358.47 $\pm$ 66.20	<0.001
TTSP (min)	443.97 $\pm$ 82.54	438.50 $\pm$ 69.40	0.002
WASO (min)	101.18 $\pm$ 71.44	80.02 $\pm$ 57.92	<0.001
Wake % of TIB	37.15 $\pm$ 15.07	31.30 $\pm$ 14.25	<0.001
ODI 3% (events h <sup>-1</sup> )	7.58 $\pm$ 10.75	6.20 $\pm$ 9.59	<0.001
ODI 4% (events h <sup>-1</sup> )	4.38 $\pm$ 7.62	3.61 $\pm$ 7.15	<0.001

## G.2 Frequent PAC vs non-frequent PAC

Table 18: Full metric comparison between frequent PAC and non-frequent PAC strata. Values are mean  $\pm$  SD.

<b>Metric</b>	<b>Frequent PAC (n=2,022)</b>	<b>Non-frequent PAC (n=8,417)</b>	<b>P-value</b>
Age (years)	68.96 $\pm$ 16.03	66.17 $\pm$ 12.20	<0.001
BMI (kg m <sup>-2</sup> )	28.08 $\pm$ 5.26	28.33 $\pm$ 5.35	0.074
AHI (events h <sup>-1</sup> )	22.09 $\pm$ 19.38	18.74 $\pm$ 16.34	<0.001
Arl (events h <sup>-1</sup> )	32.35 $\pm$ 18.85	28.69 $\pm$ 14.81	<0.001
N1 % of TST	8.00 $\pm$ 6.89	7.10 $\pm$ 6.19	<0.001
N2 % of TST	59.25 $\pm$ 11.68	57.94 $\pm$ 11.32	<0.001
N3 % of TST	14.14 $\pm$ 11.75	15.29 $\pm$ 11.37	<0.001
NREM % of TST	81.39 $\pm$ 6.95	80.33 $\pm$ 6.56	<0.001
REM % of TST	18.61 $\pm$ 6.95	19.67 $\pm$ 6.56	<0.001
SE (%)	63.67 $\pm$ 14.86	69.04 $\pm$ 14.18	<0.001
SL (min)	64.31 $\pm$ 63.75	50.37 $\pm$ 54.86	<0.001
TIB (min)	548.36 $\pm$ 81.56	528.92 $\pm$ 78.31	<0.001
TST (min)	344.11 $\pm$ 74.81	359.60 $\pm$ 65.67	<0.001
TTSP (min)	442.30 $\pm$ 79.98	438.39 $\pm$ 68.81	0.006
WASO (min)	98.19 $\pm$ 69.37	78.79 $\pm$ 57.00	<0.001
Wake % of TIB	36.33 $\pm$ 14.86	30.96 $\pm$ 14.18	<0.001
ODI 3% (events h <sup>-1</sup> )	7.86 $\pm$ 11.61	6.00 $\pm$ 9.21	<0.001
ODI 4% (events h <sup>-1</sup> )	4.61 $\pm$ 8.46	3.49 $\pm$ 6.86	<0.001

### G.3 Atrial fibrillation during sleep: AF present vs absent

Table 19: Full metric comparison between AF present and AF absent strata during sleep. Values are mean  $\pm$  SD.

<b>Metric</b>	<b>AF present (n=1,162)</b>	<b>AF absent (n=9,277)</b>	<b>P-value</b>
Age (years)	65.62 $\pm$ 19.41	66.85 $\pm$ 12.03	<0.001
BMI (kg m <sup>-2</sup> )	28.13 $\pm$ 5.34	28.30 $\pm$ 5.33	0.535
AHI (events h <sup>-1</sup> )	20.87 $\pm$ 18.79	19.21 $\pm$ 16.77	0.104
Arl (events h <sup>-1</sup> )	30.69 $\pm$ 18.20	29.24 $\pm$ 15.40	0.204
N1 % of TST	7.22 $\pm$ 6.22	7.28 $\pm$ 6.36	0.572
N2 % of TST	59.11 $\pm$ 11.90	58.08 $\pm$ 11.34	<0.001
N3 % of TST	14.77 $\pm$ 12.40	15.10 $\pm$ 11.33	0.019
NREM % of TST	81.10 $\pm$ 6.85	80.46 $\pm$ 6.62	<0.001
REM % of TST	18.90 $\pm$ 6.85	19.54 $\pm$ 6.62	<0.001
SE (%)	65.73 $\pm$ 13.87	68.28 $\pm$ 14.52	<0.001
SL (min)	63.98 $\pm$ 63.25	51.69 $\pm$ 55.96	<0.001
TIB (min)	548.11 $\pm$ 79.79	530.74 $\pm$ 79.05	<0.001
TST (min)	355.18 $\pm$ 68.35	356.78 $\pm$ 67.74	0.162
TTSP (min)	448.31 $\pm$ 74.01	437.99 $\pm$ 70.67	<0.001
WASO (min)	93.12 $\pm$ 68.13	81.22 $\pm$ 58.86	<0.001
Wake % of TIB	34.27 $\pm$ 13.87	31.72 $\pm$ 14.52	<0.001
ODI 3% (events h <sup>-1</sup> )	7.56 $\pm$ 11.51	6.21 $\pm$ 9.49	<0.001
ODI 4% (events h <sup>-1</sup> )	4.45 $\pm$ 8.42	3.61 $\pm$ 7.03	<0.001

## G.4 Ventricular tachycardia during sleep: VT present vs absent

Table 20: Full metric comparison between VT present and VT absent strata during sleep. Values are mean  $\pm$  SD.

<b>Metric</b>	<b>VT present (n=489)</b>	<b>VT absent (n=9,950)</b>	<b>P-value</b>
Age (years)	69.93 $\pm$ 15.16	66.56 $\pm$ 12.94	<0.001
BMI (kg m <sup>-2</sup> )	28.66 $\pm$ 5.91	28.26 $\pm$ 5.30	0.468
AHI (events h <sup>-1</sup> )	20.99 $\pm$ 16.74	19.32 $\pm$ 17.03	0.001
ArI (events h <sup>-1</sup> )	30.00 $\pm$ 16.49	29.37 $\pm$ 15.71	0.388
N1 % of TST	7.18 $\pm$ 5.73	7.28 $\pm$ 6.37	0.617
N2 % of TST	60.24 $\pm$ 11.70	58.10 $\pm$ 11.38	<0.001
N3 % of TST	13.57 $\pm$ 11.40	15.14 $\pm$ 11.45	<0.001
NREM % of TST	80.99 $\pm$ 6.88	80.51 $\pm$ 6.64	0.091
REM % of TST	19.01 $\pm$ 6.88	19.49 $\pm$ 6.64	0.091
SE (%)	63.26 $\pm$ 14.32	68.23 $\pm$ 14.44	<0.001
SL (min)	74.05 $\pm$ 66.62	52.04 $\pm$ 56.24	<0.001
TIB (min)	564.65 $\pm$ 81.98	531.11 $\pm$ 78.86	<0.001
TST (min)	352.44 $\pm$ 75.06	356.80 $\pm$ 67.43	0.217
TTSP (min)	454.35 $\pm$ 78.17	438.40 $\pm$ 70.68	<0.001
WASO (min)	101.91 $\pm$ 69.93	81.60 $\pm$ 59.40	<0.001
Wake % of TIB	36.74 $\pm$ 14.32	31.77 $\pm$ 14.44	<0.001
ODI 3% (events h <sup>-1</sup> )	7.68 $\pm$ 10.32	6.30 $\pm$ 9.72	<0.001
ODI 4% (events h <sup>-1</sup> )	4.43 $\pm$ 7.33	3.67 $\pm$ 7.20	<0.001

## G.5 Median-split stratification by nocturnal mean heart rate

Table 21: Full metric comparison between strata defined by the median nocturnal mean heart rate (64 bpm): high HR ( $\geq 64$  bpm) vs low HR ( $< 64$  bpm). Values are mean  $\pm$  SD. Overall, differences across most sleep phenotypes were modest under this stratification, suggesting limited discriminative utility of nocturnal mean heart rate alone in the pooled multi-cohort sample. Given the substantial burden of sleep disturbances in the included cohorts, mean heart rate may reflect multiple interacting sleep- and cardiovascular-related factors, thereby reducing the specificity of a single-variable partition. Stratification by nocturnal maximum and minimum heart rate similarly did not yield more distinctive sleep-phenotype separation.

Metric	High HR ( $\geq 64$ ) (n=5301)	Low HR ( $< 64$ ) (n=5138)	P-value
Age (years)	64.80 $\pm$ 13.65	68.69 $\pm$ 12.14	<0.001
BMI (kg m <sup>-2</sup> )	28.86 $\pm$ 5.77	27.68 $\pm$ 4.77	<0.001
AHI (events h <sup>-1</sup> )	20.01 $\pm$ 18.07	18.76 $\pm$ 15.84	0.087
Arl (events h <sup>-1</sup> )	29.58 $\pm$ 16.42	29.21 $\pm$ 15.01	0.695
N1 % of TST	7.30 $\pm$ 6.56	7.25 $\pm$ 6.10	0.292
N2 % of TST	57.79 $\pm$ 11.81	58.62 $\pm$ 10.96	<0.001
N3 % of TST	15.75 $\pm$ 11.79	14.36 $\pm$ 11.06	<0.001
NREM % of TST	80.84 $\pm$ 6.74	80.22 $\pm$ 6.55	<0.001
REM % of TST	19.16 $\pm$ 6.74	19.78 $\pm$ 6.55	<0.001
SE (%)	68.33 $\pm$ 14.77	67.65 $\pm$ 14.15	<0.001
SL (min)	51.47 $\pm$ 55.00	54.72 $\pm$ 58.87	0.025
TIB (min)	526.84 $\pm$ 76.27	538.72 $\pm$ 81.92	<0.001
TST (min)	354.87 $\pm$ 70.07	358.38 $\pm$ 65.35	0.081
TTSP (min)	435.02 $\pm$ 71.77	443.41 $\pm$ 70.20	<0.001
WASO (min)	80.15 $\pm$ 60.39	85.03 $\pm$ 59.68	<0.001
Wake % of TIB	31.67 $\pm$ 14.77	32.35 $\pm$ 14.15	<0.001
ODI 3% (events h <sup>-1</sup> )	6.81 $\pm$ 10.62	5.90 $\pm$ 8.74	<0.001
ODI 4% (events h <sup>-1</sup> )	4.04 $\pm$ 7.94	3.36 $\pm$ 6.34	<0.001

## G.6 HRV quantile-based stratification: SDANN as an example

Table 22: Full metric comparison between HRV strata defined by SDANN quantiles: high SDANN (P75;  $\geq 198.19$ ) vs low SDANN (P25;  $\leq 114.15$ ). Values are mean  $\pm$  SD. HRV candidates considered in this study included SDNN, SDANN, SDANNIndex, RMSSD, pNN50, HRV triangular index (HRV\_tri), LF, HF, LFnu, HFnu, and LF/HF; SDANN is reported here as a representative example. Although some comparisons yield small P-values, between-stratum differences in means and the corresponding variability across most sleep phenotypes are generally modest, suggesting limited discriminative separation when stratifying by a single HRV metric alone in the pooled sample.

Metric	High SDANN ( $\geq 198.19$ ) (n=2,609)	Low SDANN ( $\leq 114.15$ ) (n=2,610)	P-value
Age (years)	68.38 $\pm$ 12.35	65.17 $\pm$ 13.90	<0.001
BMI (kg m <sup>-2</sup> )	27.84 $\pm$ 5.11	28.90 $\pm$ 5.93	<0.001
AHI (events h <sup>-1</sup> )	19.08 $\pm$ 16.73	19.71 $\pm$ 17.55	0.394
Arl (events h <sup>-1</sup> )	29.23 $\pm$ 15.55	29.44 $\pm$ 16.04	0.776
N1 % of TST	6.87 $\pm$ 5.77	7.25 $\pm$ 6.76	0.360
N2 % of TST	58.33 $\pm$ 11.27	58.28 $\pm$ 11.92	0.972
N3 % of TST	15.13 $\pm$ 11.52	15.45 $\pm$ 11.75	0.352
NREM % of TST	80.32 $\pm$ 6.57	80.99 $\pm$ 6.67	<0.001
REM % of TST	19.68 $\pm$ 6.57	19.01 $\pm$ 6.67	<0.001
SE (%)	66.90 $\pm$ 14.18	69.60 $\pm$ 14.95	<0.001
SL (min)	52.99 $\pm$ 57.29	50.50 $\pm$ 54.52	0.172
TIB (min)	538.68 $\pm$ 82.20	521.79 $\pm$ 74.35	<0.001
TST (min)	354.52 $\pm$ 66.65	357.98 $\pm$ 69.73	0.002
TTSP (min)	437.33 $\pm$ 72.70	438.47 $\pm$ 69.53	0.269
WASO (min)	82.81 $\pm$ 60.14	80.49 $\pm$ 59.51	0.121
Wake % of TIB	33.10 $\pm$ 14.18	30.40 $\pm$ 14.95	<0.001
ODI 3% (events h <sup>-1</sup> )	6.33 $\pm$ 9.40	6.60 $\pm$ 10.27	0.615
ODI 4% (events h <sup>-1</sup> )	3.70 $\pm$ 6.94	3.88 $\pm$ 7.55	0.626

---

## Pittsburgh Sleep Quality Index (PSQI)

# 67

**Purpose** As psychiatric disorders are often associated with sleep disturbances, the PSQI was designed to evaluate overall sleep quality in these clinical populations. Each of the questionnaire's 19 self-reported items belongs to one of seven subcategories: subjective sleep quality, sleep latency, sleep duration, habitual sleep efficiency, sleep disturbances, use of sleeping medication, and daytime dysfunction. Five additional questions rated by the respondent's roommate or bed partner are included for clinical purposes and are not scored.

**Population for Testing** The developers' initial psychometric analysis of the instrument was conducted with individuals aged 24–83 years [1]. The questionnaire has been validated with a variety of clinical populations, including: patients with major depressive disorder, disorders of initiating and maintaining sleep, disorders of excessive somnolence, cancer [2], and fibromyalgia [3].

**Administration** A self-report, pencil-and-paper measure, the instrument should require between 5 and 10 min for completion.

**Reliability and Validity** Though there have been a variety of studies assessing the psychometric properties of the scale, the developers'

initial evaluation [1] found an internal reliability of  $\alpha=.83$ , a test–retest reliability of .85 for the global scale, a sensitivity of 89.6%, and a specificity of 86.5%.

**Obtaining a Copy** A copy can be found in the original article published by developers [1].

Direct correspondence to:  
Dr. C.F. Reynolds  
Western Psychiatric Institute and Clinic, University of Pittsburgh  
3811 O'Hara St.  
Pittsburgh, PA 15213, USA

**Scoring** A detailed guide to scoring is included in the original published article [1]. The questionnaire consists of a combination of Likert-type and open-ended questions (later converted to scaled scores using provided guidelines). Respondents are asked to indicate how frequently they have experienced certain sleep difficulties over the past month and to rate their overall sleep quality. Scores for each question range from 0 to 3, with higher scores indicating more acute sleep disturbances. Developers have suggested a cut-off score of 5 for the global scale as it correctly identified 88.5% of the patient group in their validation study.

Subject's Initials \_\_\_\_\_ ID# \_\_\_\_\_ Date \_\_\_\_\_ Time \_\_\_\_\_ AM  
PM

**PITTSBURGH SLEEP QUALITY INDEX**

**INSTRUCTIONS:**

The following questions relate to your usual sleep habits during the past month only. Your answers should indicate the most accurate reply for the majority of days and nights in the past month. Please answer all questions.

1. During the past month, what time have you usually gone to bed at night?  
BED TIME \_\_\_\_\_
2. During the past month, how long (in minutes) has it usually taken you to fall asleep each night?  
NUMBER OF MINUTES \_\_\_\_\_
3. During the past month, what time have you usually gotten up in the morning?  
GETTING UP TIME \_\_\_\_\_
4. During the past month, how many hours of actual sleep did you get at night? (This may be different than the number of hours you spent in bed.)  
HOURS OF SLEEP PER NIGHT \_\_\_\_\_

***For each of the remaining questions, check the one best response. Please answer all questions.***

5. During the past month, how often have you had trouble sleeping because you . . .
  - a) Cannot get to sleep within 30 minutes
 

Not during the past month _____	Less than once a week _____	Once or twice a week _____	Three or more times a week _____
------------------------------------	--------------------------------	-------------------------------	-------------------------------------
  - b) Wake up in the middle of the night or early morning
 

Not during the past month _____	Less than once a week _____	Once or twice a week _____	Three or more times a week _____
------------------------------------	--------------------------------	-------------------------------	-------------------------------------
  - c) Have to get up to use the bathroom
 

Not during the past month _____	Less than once a week _____	Once or twice a week _____	Three or more times a week _____
------------------------------------	--------------------------------	-------------------------------	-------------------------------------

d) Cannot breathe comfortably

Not during the past month _____	Less than once a week _____	Once or twice a week _____	Three or more times a week _____
------------------------------------	--------------------------------	-------------------------------	-------------------------------------

e) Cough or snore loudly

Not during the past month _____	Less than once a week _____	Once or twice a week _____	Three or more times a week _____
------------------------------------	--------------------------------	-------------------------------	-------------------------------------

f) Feel too cold

Not during the past month _____	Less than once a week _____	Once or twice a week _____	Three or more times a week _____
------------------------------------	--------------------------------	-------------------------------	-------------------------------------

g) Feel too hot

Not during the past month _____	Less than once a week _____	Once or twice a week _____	Three or more times a week _____
------------------------------------	--------------------------------	-------------------------------	-------------------------------------

h) Had bad dreams

Not during the past month _____	Less than once a week _____	Once or twice a week _____	Three or more times a week _____
------------------------------------	--------------------------------	-------------------------------	-------------------------------------

i) Have pain

Not during the past month _____	Less than once a week _____	Once or twice a week _____	Three or more times a week _____
------------------------------------	--------------------------------	-------------------------------	-------------------------------------

j) Other reason(s), please describe \_\_\_\_\_

---

How often during the past month have you had trouble sleeping because of this?

Not during the past month _____	Less than once a week _____	Once or twice a week _____	Three or more times a week _____
------------------------------------	--------------------------------	-------------------------------	-------------------------------------

6. During the past month, how would you rate your sleep quality overall?

Very good \_\_\_\_\_

Fairly good \_\_\_\_\_

Fairly bad \_\_\_\_\_

Very bad \_\_\_\_\_

7. During the past month, how often have you taken medicine to help you sleep (prescribed or "over the counter")?

Not during the past month \_\_\_\_\_ Less than once a week \_\_\_\_\_ Once or twice a week \_\_\_\_\_ Three or more times a week \_\_\_\_\_

8. During the past month, how often have you had trouble staying awake while driving, eating meals, or engaging in social activity?

Not during the past month \_\_\_\_\_ Less than once a week \_\_\_\_\_ Once or twice a week \_\_\_\_\_ Three or more times a week \_\_\_\_\_

9. During the past month, how much of a problem has it been for you to keep up enough enthusiasm to get things done?

No problem at all \_\_\_\_\_

Only a very slight problem \_\_\_\_\_

Somewhat of a problem \_\_\_\_\_

A very big problem \_\_\_\_\_

10. Do you have a bed partner or room mate?

No bed partner or room mate \_\_\_\_\_

Partner/room mate in other room \_\_\_\_\_

Partner in same room, but not same bed \_\_\_\_\_

Partner in same bed \_\_\_\_\_

If you have a room mate or bed partner, ask him/her how often in the past month you have had . . .

- a) Loud snoring

Not during the past month \_\_\_\_\_ Less than once a week \_\_\_\_\_ Once or twice a week \_\_\_\_\_ Three or more times a week \_\_\_\_\_

- b) Long pauses between breaths while asleep

Not during the past month \_\_\_\_\_ Less than once a week \_\_\_\_\_ Once or twice a week \_\_\_\_\_ Three or more times a week \_\_\_\_\_

- c) Legs twitching or jerking while you sleep

Not during the past month \_\_\_\_\_ Less than once a week \_\_\_\_\_ Once or twice a week \_\_\_\_\_ Three or more times a week \_\_\_\_\_

## d) Episodes of disorientation or confusion during sleep

Not during the past month \_\_\_\_\_    Less than once a week \_\_\_\_\_    Once or twice a week \_\_\_\_\_    Three or more times a week \_\_\_\_\_

## e) Other restlessness while you sleep; please describe \_\_\_\_\_

Not during the past month \_\_\_\_\_    Less than once a week \_\_\_\_\_    Once or twice a week \_\_\_\_\_    Three or more times a week \_\_\_\_\_

This form may only be used for non-commercial education and research purposes. If you would like to use this instrument for commercial purposes or for commercially sponsored research, please contact the Office of Technology Management at the University of Pittsburgh at 412-648-2206 for licensing information.

Copyright 1989 and 2010, University of Pittsburgh. All rights reserved. Developed by [1] of the University of Pittsburgh using National Institute of Mental Health Funding.

Buyse et al. [1].

---

## References

1. Buyse, D. J., Reynolds, C. F., Charles, F., Monk, T. H., Berman, S. R., & Kupfer, D. J. (1989). The Pittsburgh sleep quality index: a new instrument for psychiatric practice and research. *Psychiatry Research*, *28*(2), 193–213.
2. Dudley, W. N. (2004). Psychometric evaluation of the Pittsburgh sleep quality index in cancer patients. *Journal of Pain and Symptom Management*, *27*(2), 140–148.
3. Osorio, C. D., Gallinaro, A. L., Lorenzi-Filho, G., & Lage, L. G. (2006). Sleep quality in patients with fibromyalgia using the Pittsburgh sleep quality index. *Journal of Rheumatology*, *33*(9), 1863–1865.

---

## Representative Studies Using Scale

- Dolberg, O. T., Hirschmann, S., & Grunhaus, L. (1998). Melatonin for the treatment of sleep disturbances in major depressive disorder. *American Journal of Psychiatry*, *155*, 1119–1121.
- Jennings, J. R., Muldoon, M. F., Hall, M., Buyse, D. J., & Manuck, S. B. (2007). Self-reported sleep quality is associated with the metabolic structure. *Sleep*, *30*(2), 219–223.